Magnetic Activity in the Galactic Centre Region

Suzuki, T. K.

Arts & Sciences, U.Tokyo

Dec. 22nd, 2017

Suzuki, Fukui, Torii, Machida, & Matsumoto 2015 MNRAS, 454, 3049
Kakiuchi, Suzuki, Fukui, Torii, Machida, & Matsumoto 2017 (arxiv:171204209)
Suzuki & Lazarian 2017 (arxiv:171003930)
Thanks to PC clusters(Ta lab.), Cray XC30 (NAOJ), HITACHI SR16000(Yukawa inst.)

Outline

Roles of Magnetic Field in the Galactic Centre Region (10 pc ~ 1 kpc) on Complex Flows

- Radial Flows
  - –Parallelogram in an $l - v$ diagram
- Outflows
  - –Relation to the Fermi Bubbles?

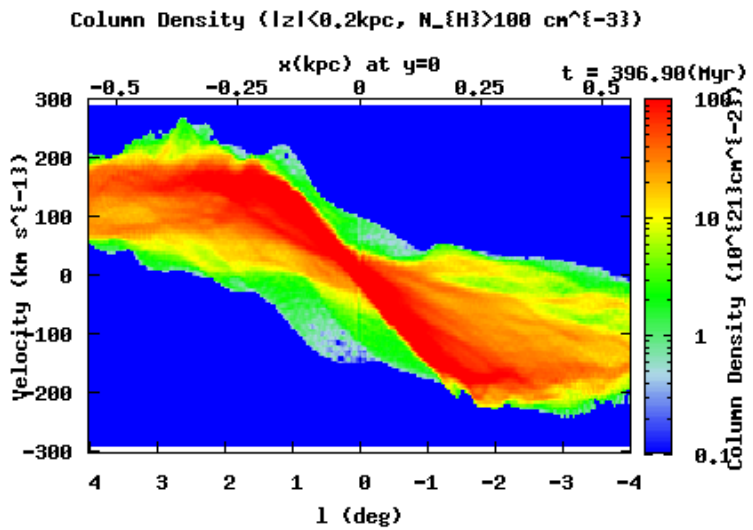

Galactic l–v diagram

Galactic l–v diagram

CO(J=1-0) Dame+ 2001
(Rodriguez-Fernandez & Combes 2008)

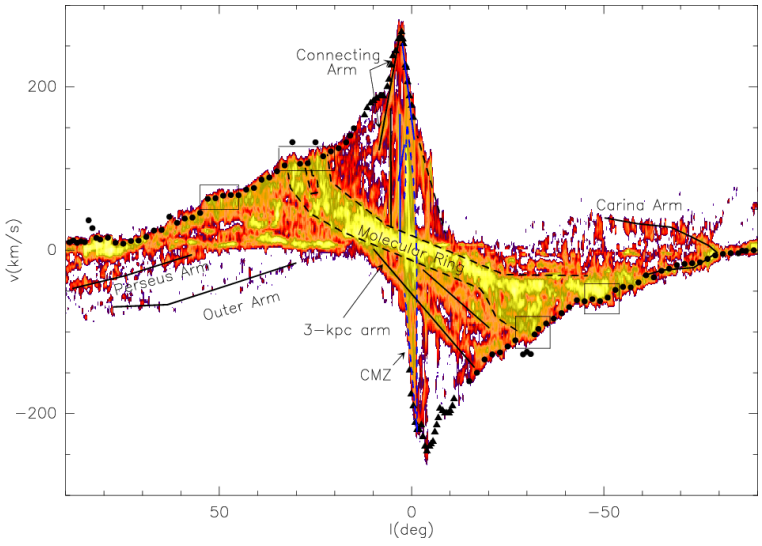

Galactic *l*–*v* diagram

CO(J=1-0) Dame+ 2001
(Rodriguez-Fernandez & Combes 2008)

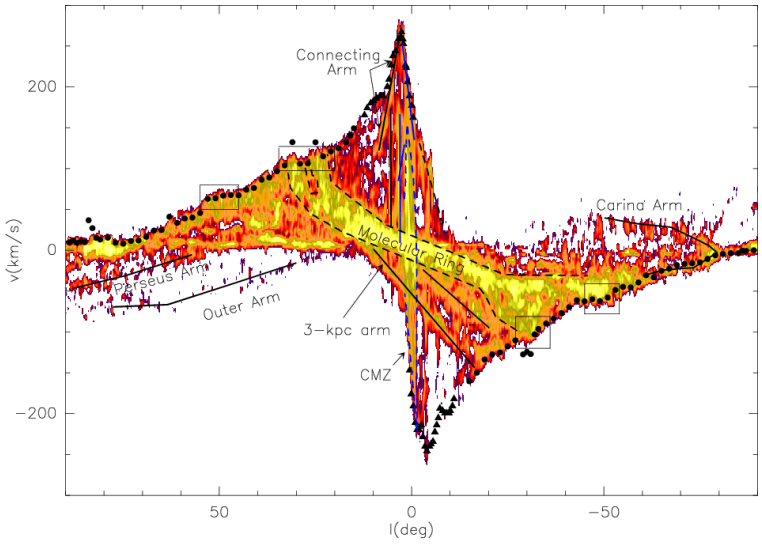

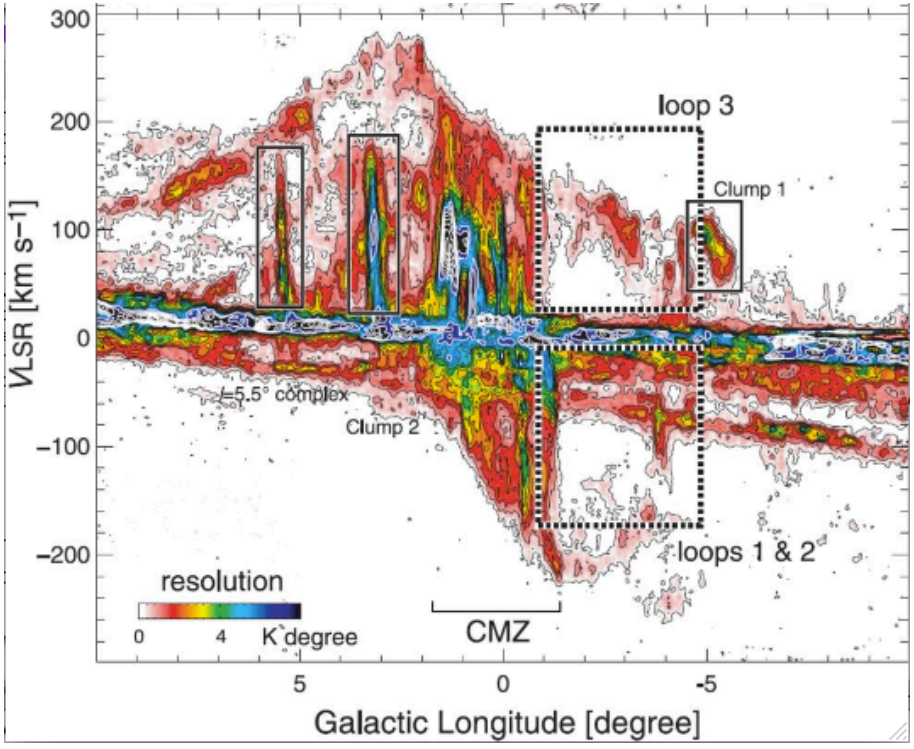

^{12}CO(J=1-0) by NANTEN

Torii+ 2010

Galactic *l–v* diagram

CO(J=1-0) Dame+ 2001
(Rodriguez-Fernandez & Combes 2008)

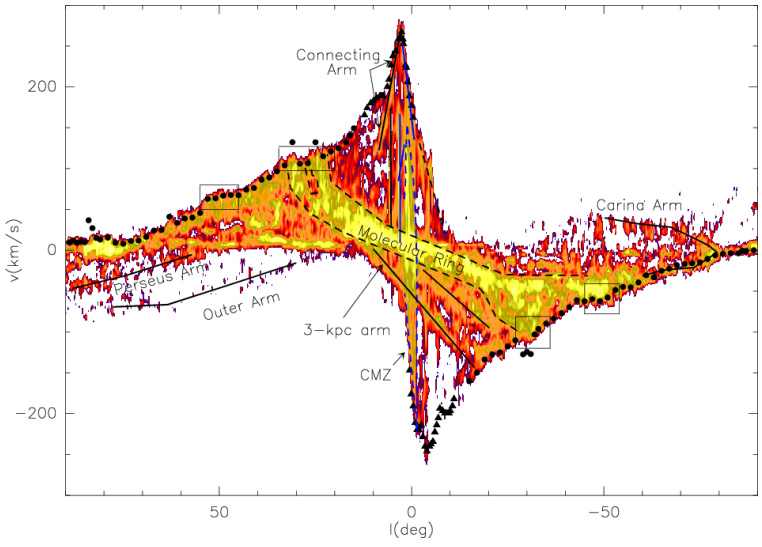

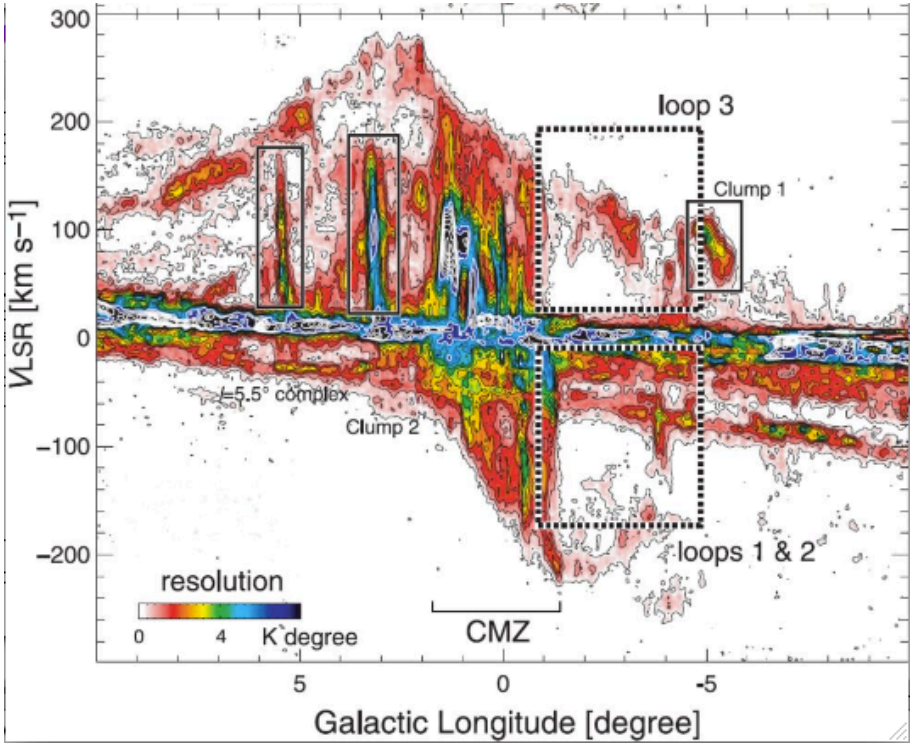

^{12}CO(J=1-0) by NANTEN
Torii+ 2010

asymmetric “Parallelogram”
in the *l–v* diagram

Galactic *l–v* diagram

CO(J=1-0) Dame+ 2001
(Rodriguez-Fernandez & Combes 2008)

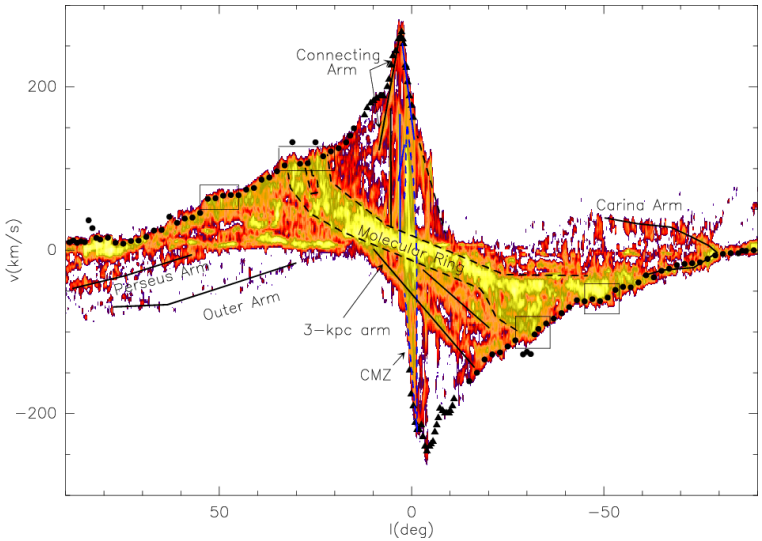

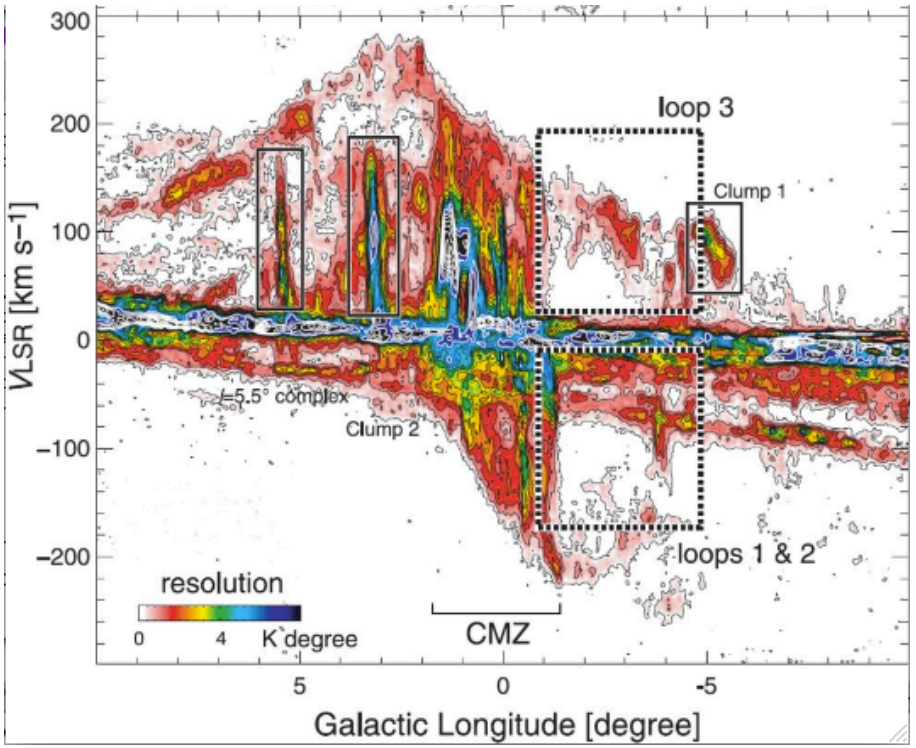

c.f. Circular motion

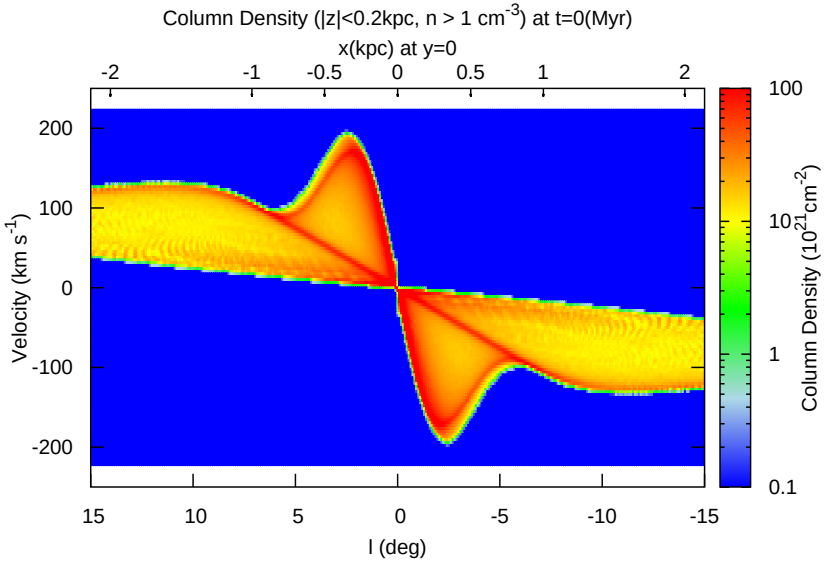

^{12}CO(J=1-0) by NANTEN

Torii+ 2010

asymmetric “Parallelogram”
in the *l–v* diagram

Galactic *l–v* diagram

CO(J=1-0) Dame+ 2001
(Rodriguez-Fernandez & Combes 2008)

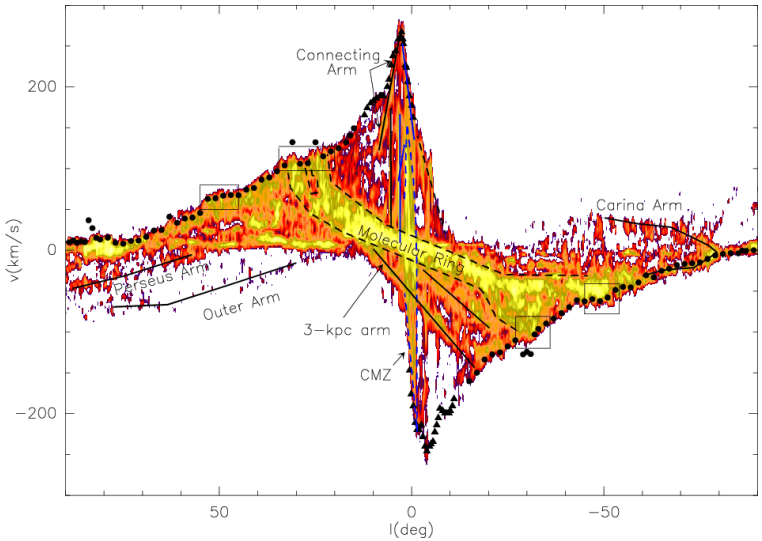

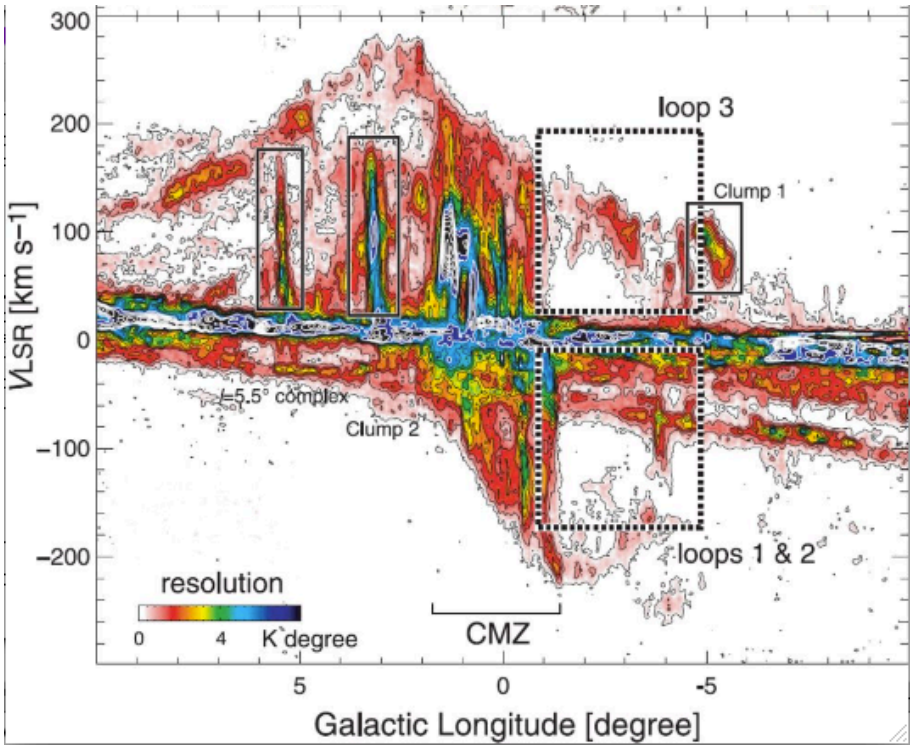

c.f. Circular motion

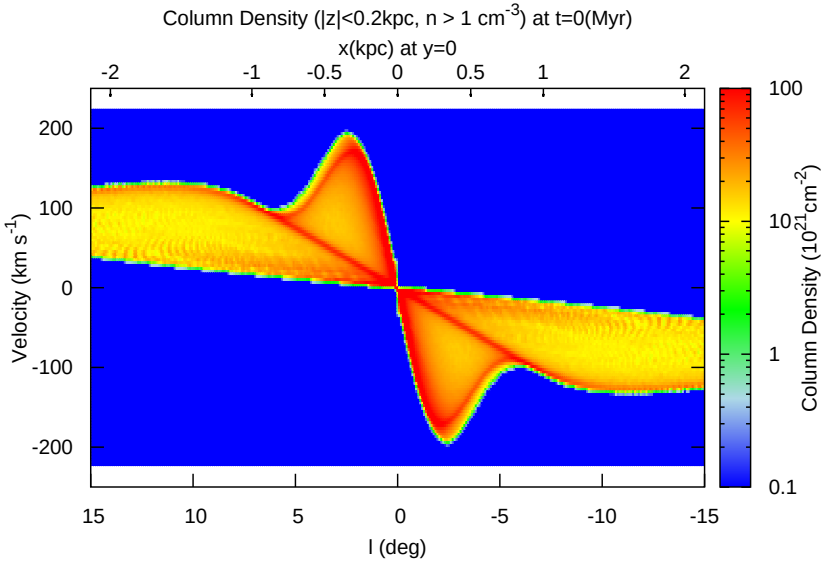

^{12}CO(J=1-0) by NANTEN
Torii+ 2010

asymmetric “Parallelogram”
in the *l–v* diagram
⇒ Non-circular motion

Bar⇔ Non-circular Motion?

Bar⇔ Non-circular Motion?

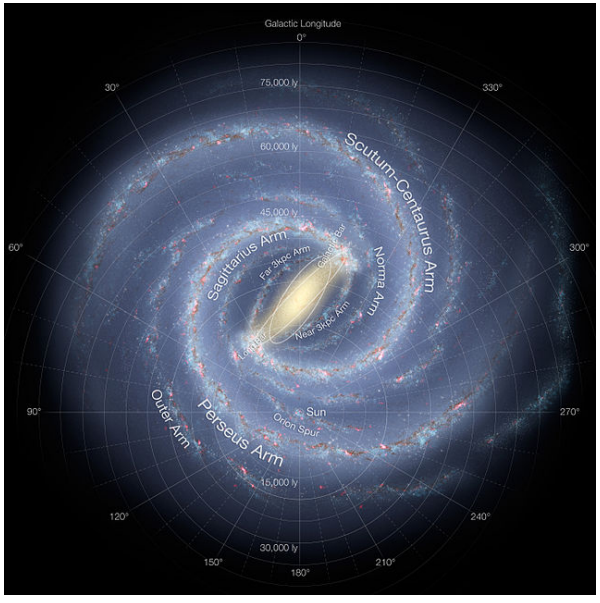

Artistic view (NASA JPL)

Stellar Bar⇐IR obs.

Okuda+ 1977; Hayakawa+ 1981;
Matsumoto+ 1982;
Blitz & Spergel 1991; Churchwell+ 2009

Bar⇔ Non-circular Motion?

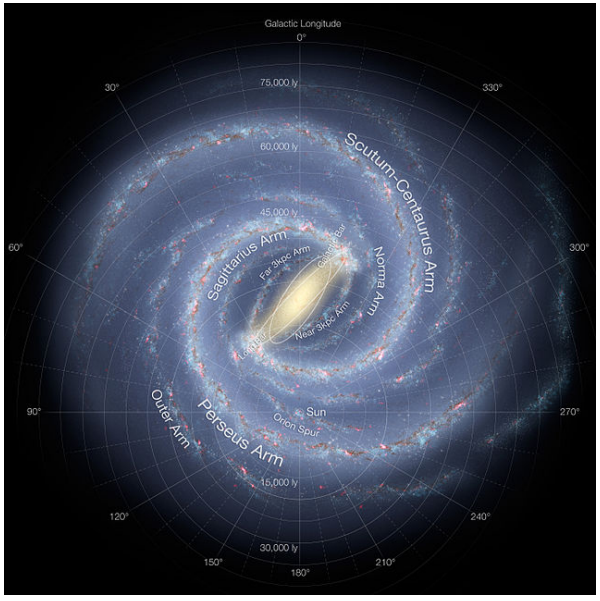

Artistic view (NASA JPL)

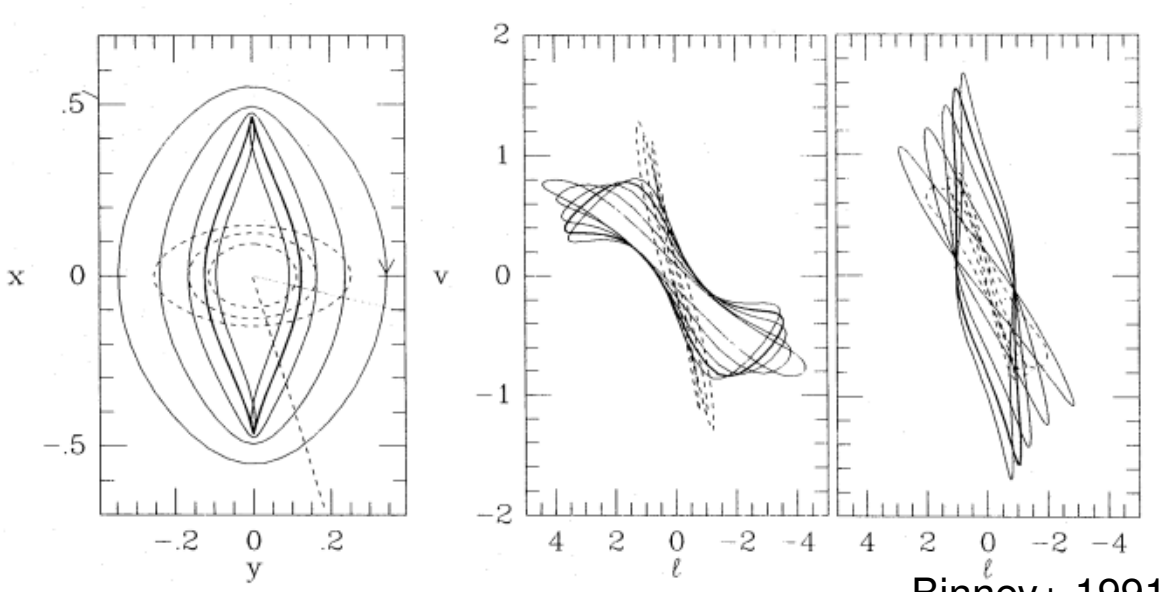

Binney+ 1991

Stellar Bar⇐IR obs.

Okuda+ 1977; Hayakawa+ 1981;
Matsumoto+ 1982;
Blitz & Spergel 1991; Churchwell+ 2009

Bar⇔ Non-circular Motion?

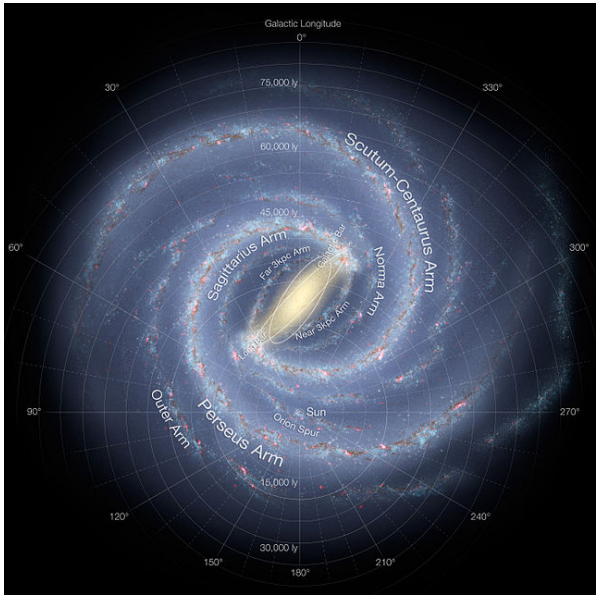

Artistic view (NASA JPL)

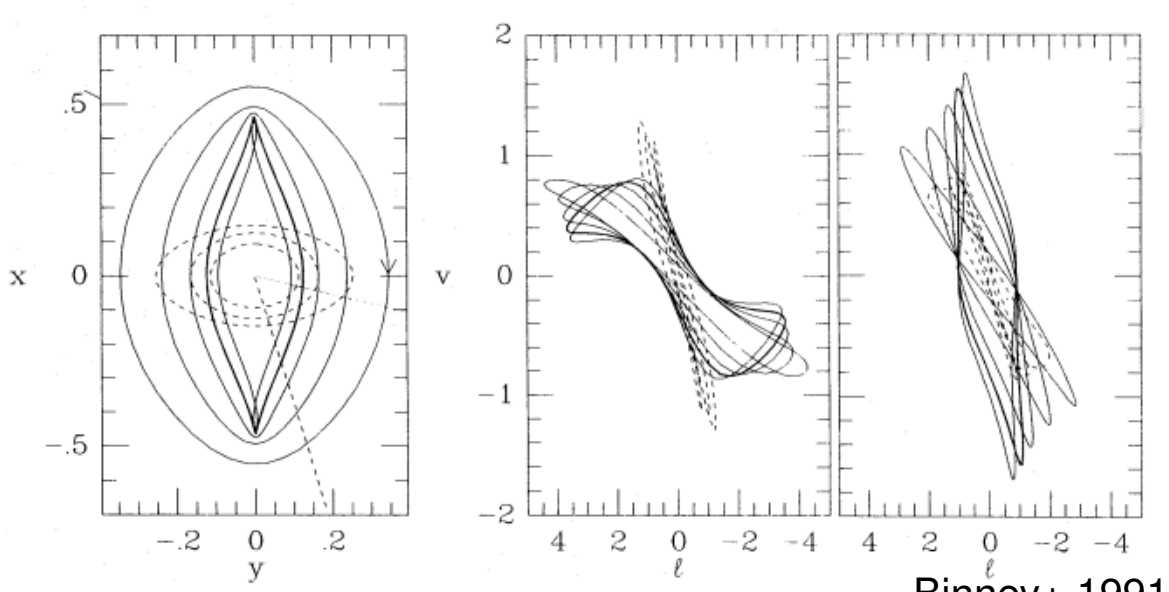

Binney+ 1991

Observe a bar from an oblique angle

Stellar Bar⇐IR obs.

Okuda+ 1977; Hayakawa+ 1981;
Matsumoto+ 1982;
Blitz & Spergel 1991; Churchwell+ 2009

Bar⇔ Non-circular Motion?

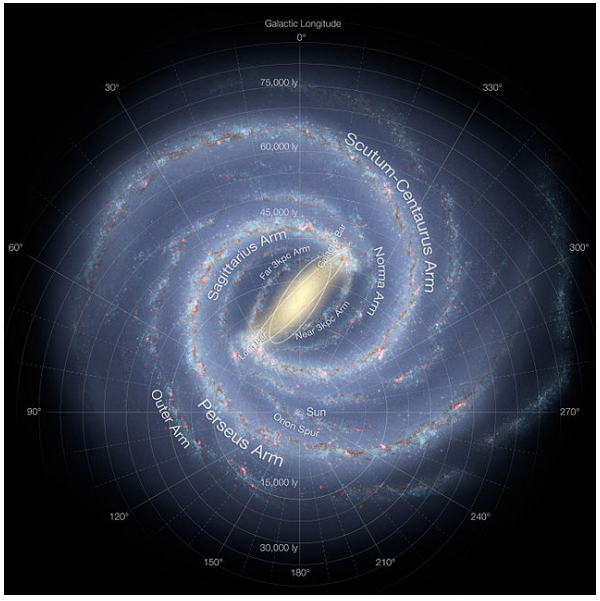

Artistic view (NASA JPL)

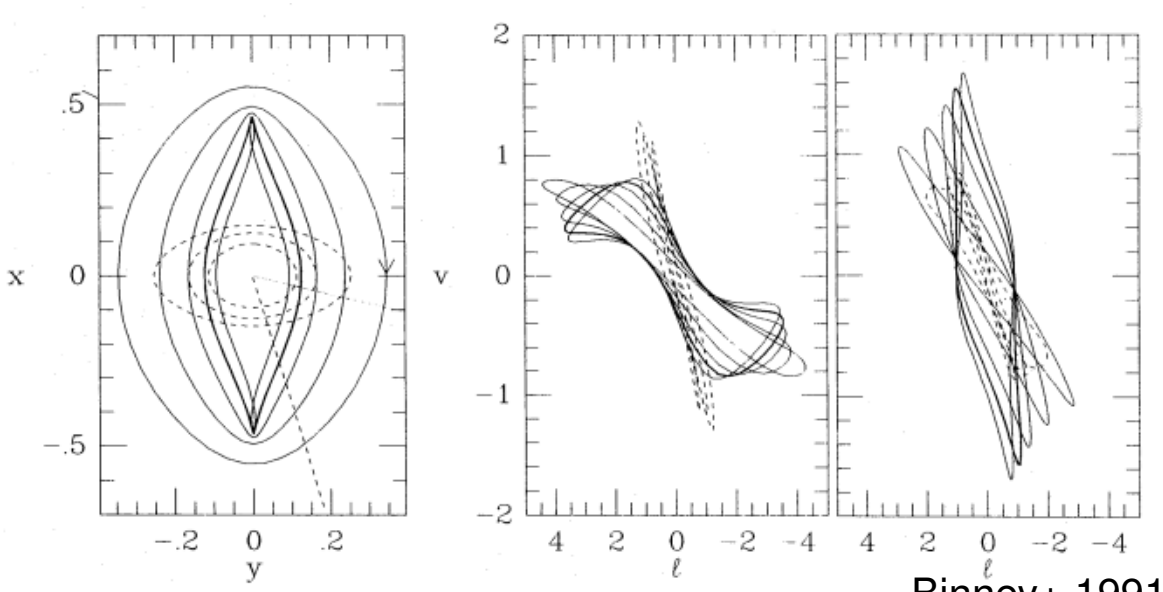

Binney+ 1991

Observe a bar from an oblique angle

⇒ symmetric Parallelogram

Stellar Bar⇐IR obs.

Okuda+ 1977; Hayakawa+ 1981; Matsumoto+ 1982; Blitz & Spergel 1991; Churchwell+ 2009

Bar⇔ Non-circular Motion?

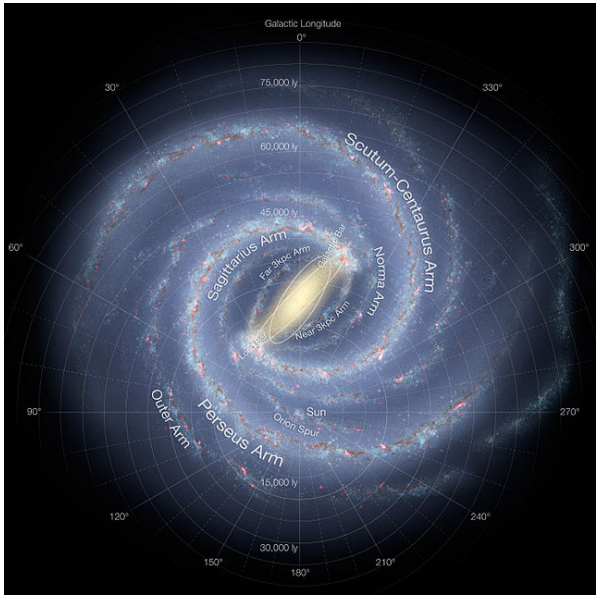

Artistic view (NASA JPL)

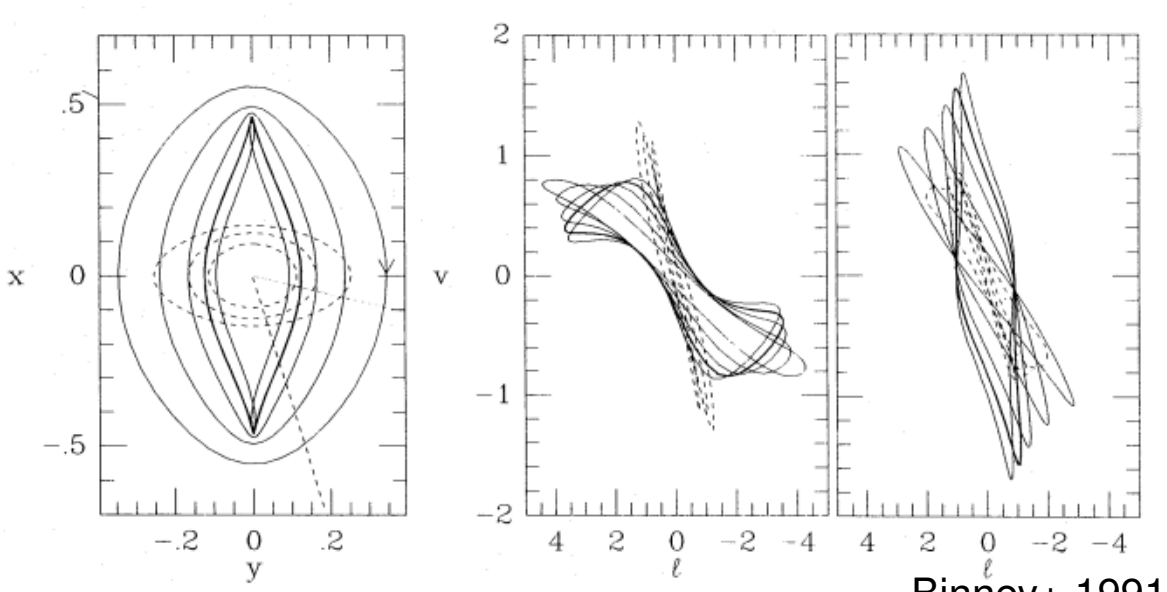

Binney+ 1991

Observe a bar from an oblique angle

⇒ symmetric Parallelogram

Stellar Bar⇐IR obs.

Okuda+ 1977; Hayakawa+ 1981; Matsumoto+ 1982; Blitz & Spergel 1991; Churchwell+ 2009

Many works with a bar potential

Koda & Wada 2002; Baba+ 2010; Molinari+ 2011; Shin & Kim 2015

Magnetic Fields

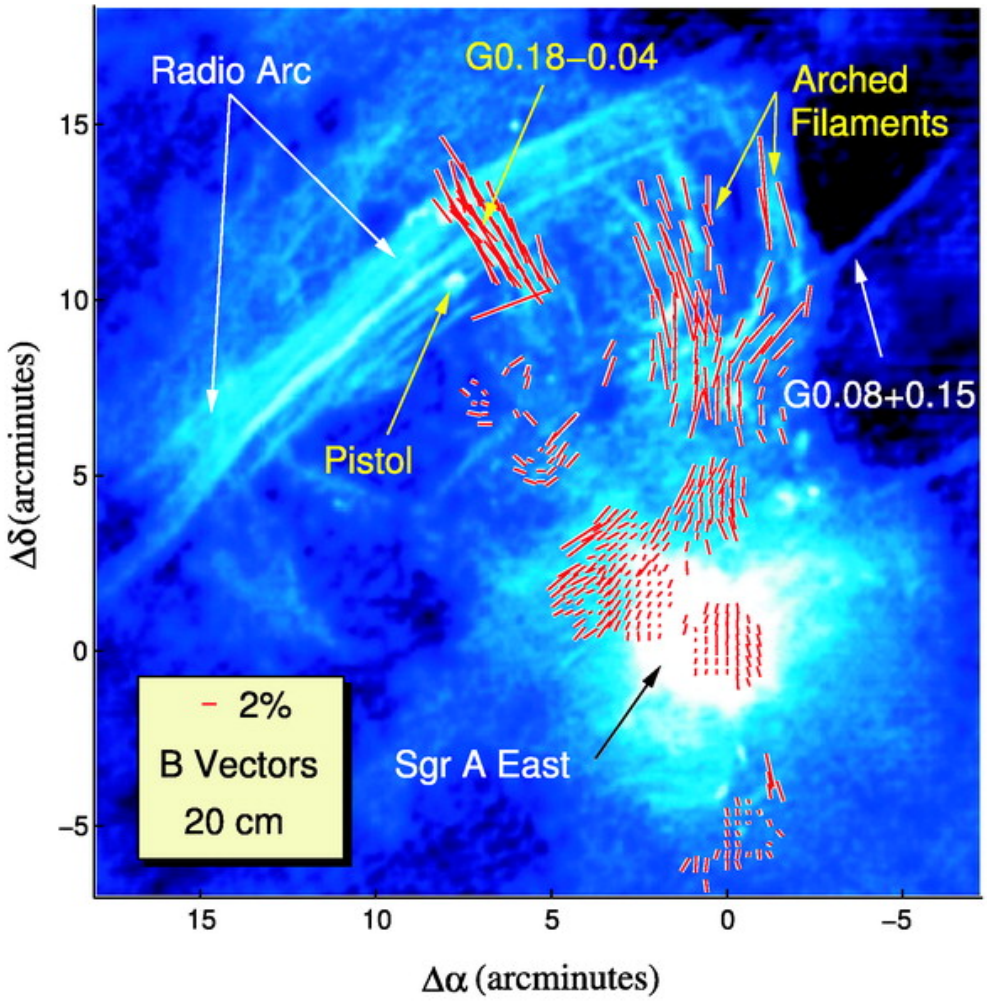

Chuss+ 2003

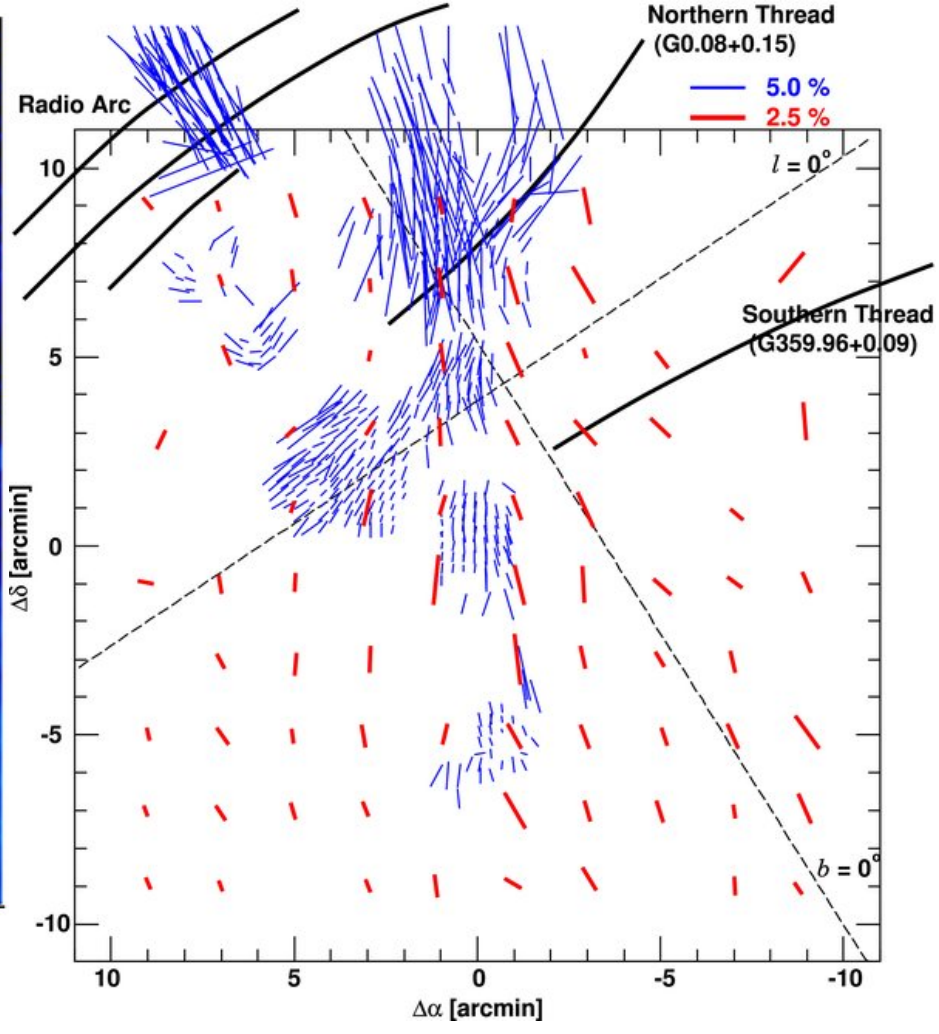

Nishiyama+ 2010

– inferred B fields

from FIR/sub-mm polariztion

– from IR pol. by IRSF

Caveat: $A_V \approx 3$ mag.

Magnetic Field –contd.

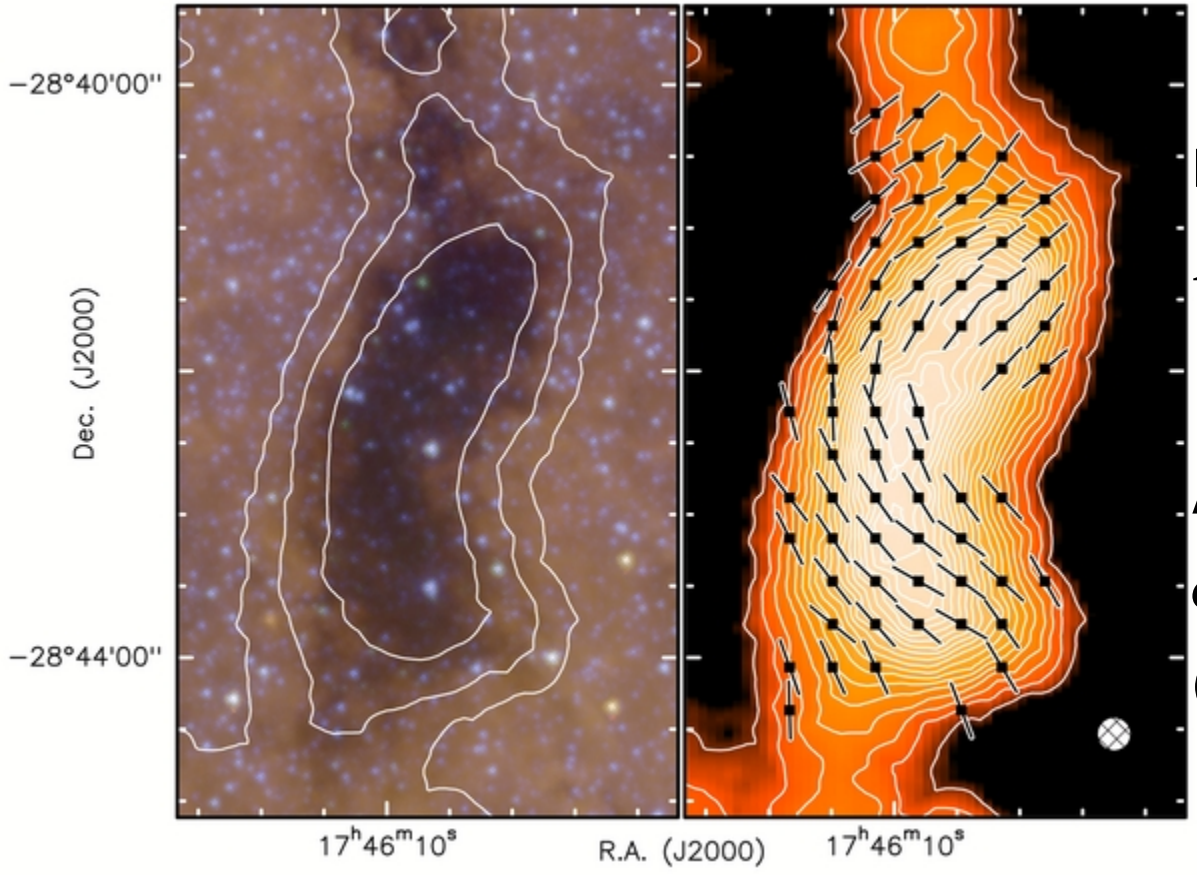

Pillai+ 2015

$B \sim 5$ mG

Assuming

$\delta B / \sqrt{\rho} \approx \delta v$

(Chandrasekhar & Fermi method)

Magnetic Loops

Magnetic Loops

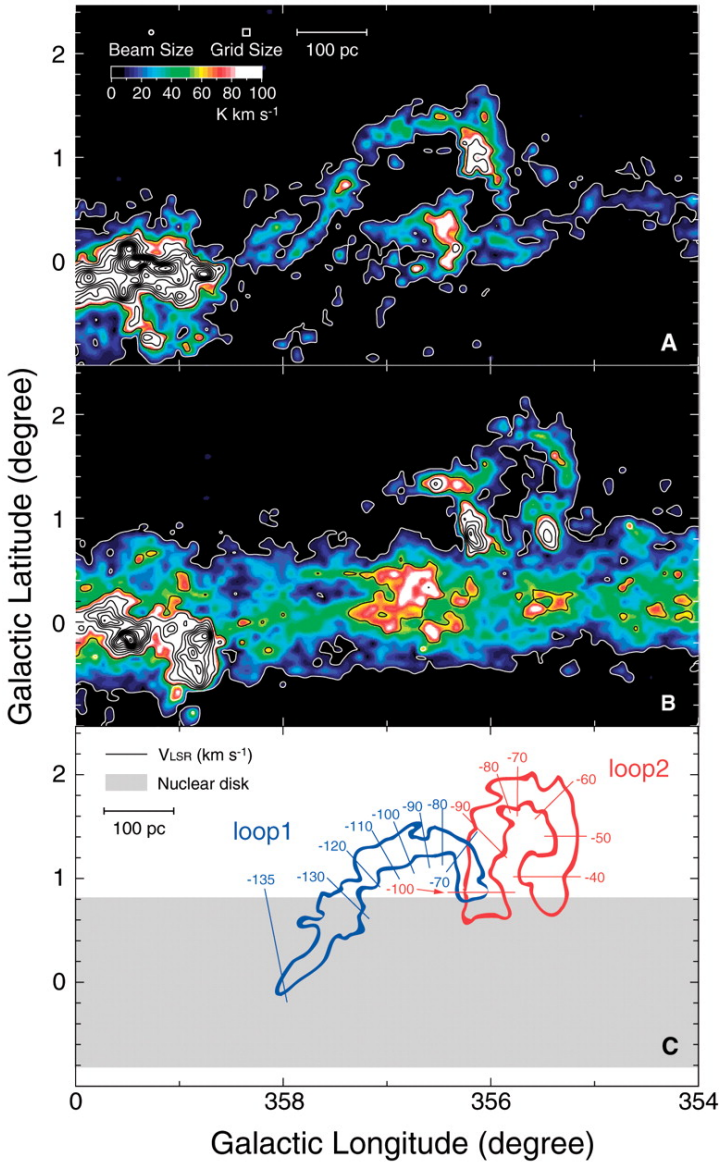

Fukui+ 2006

Magnetic Loops

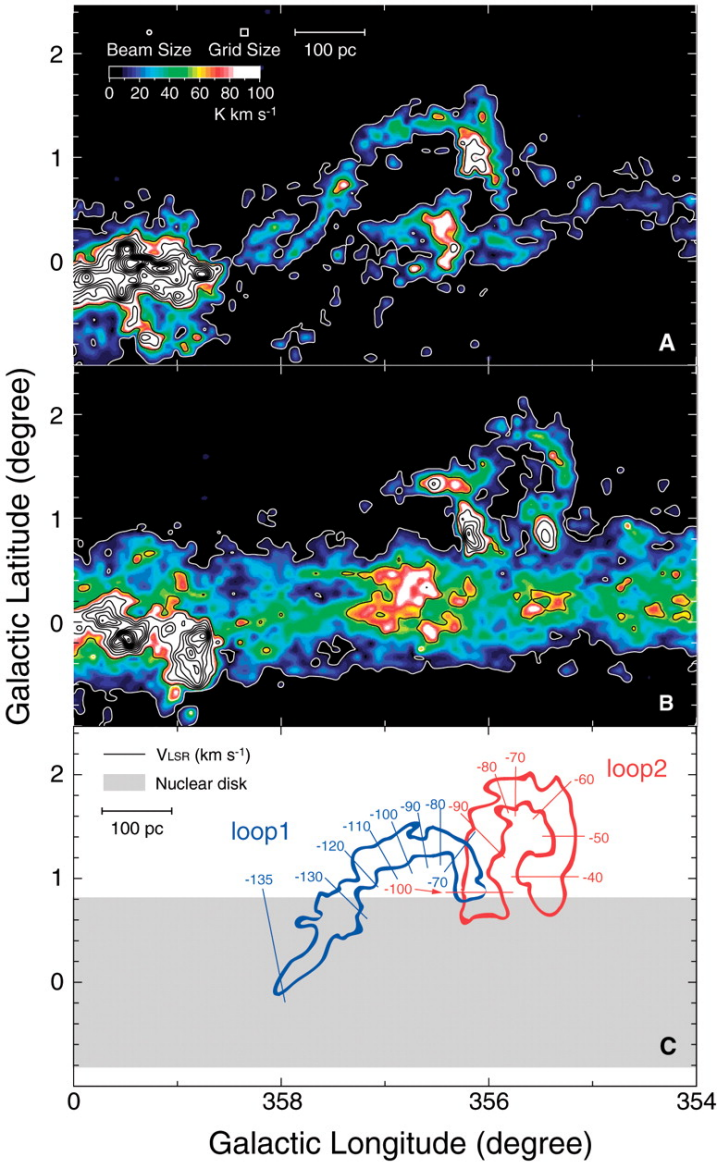

Fukui+ 2006

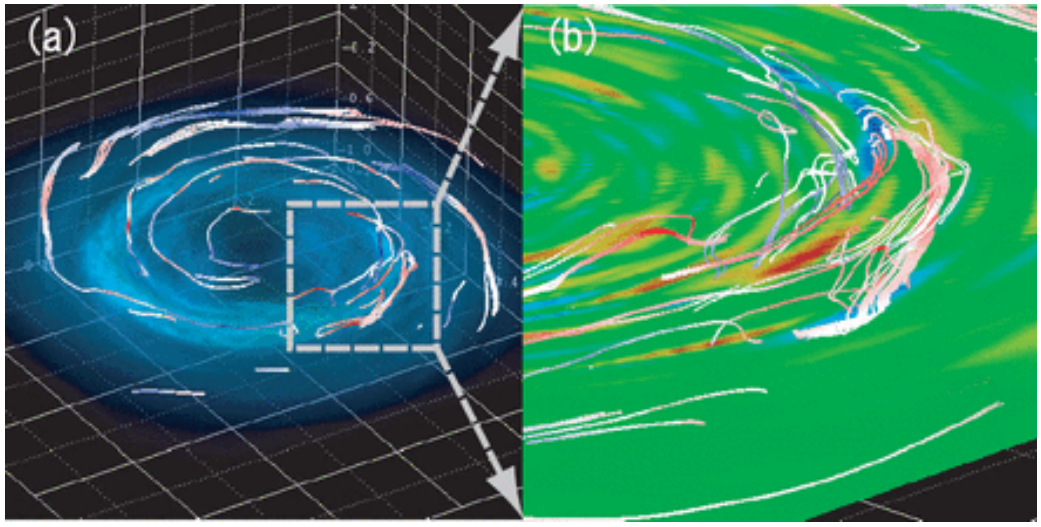

Machida+ 2009

Magnetic Loops

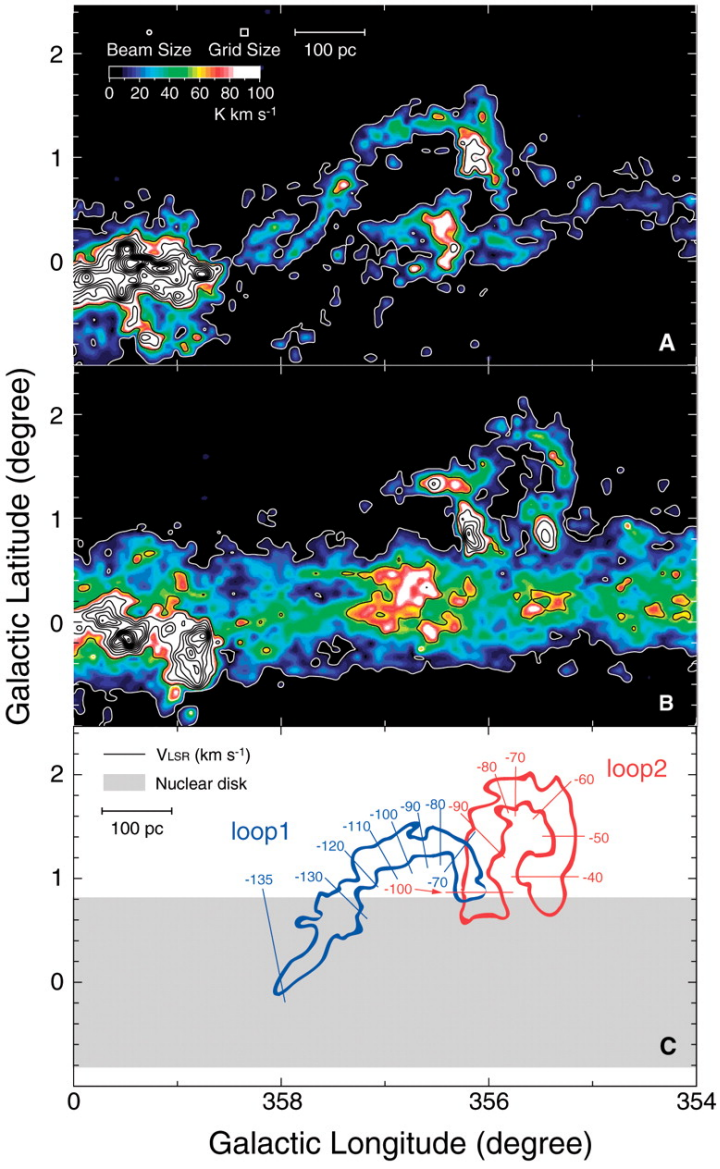

Fukui+ 2006

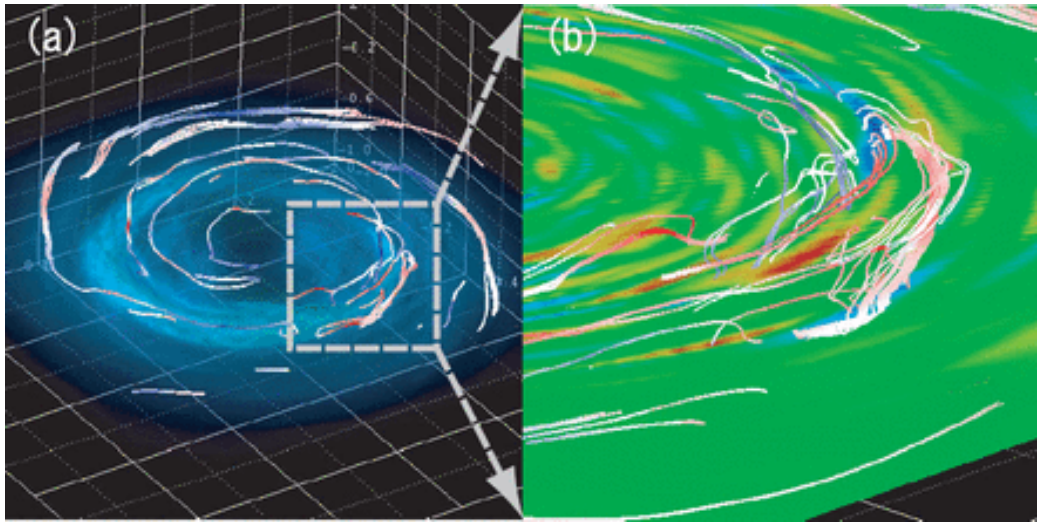

Machida+ 2009

Parker Instability (Mag. Buoyancy)

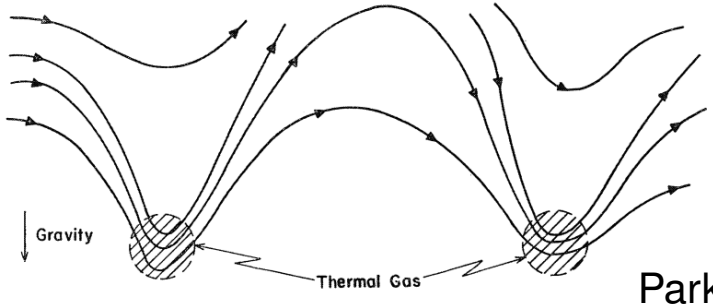

Parker 1966

FIG 2.—Sketch of the local state of the lines of force of the interstellar magnetic field and interstellar gas-cloud configuration resulting from the intrinsic instability of a large-scale field along the galactic disk or arm when confined by the weight of the gas.

Magnetic Loops

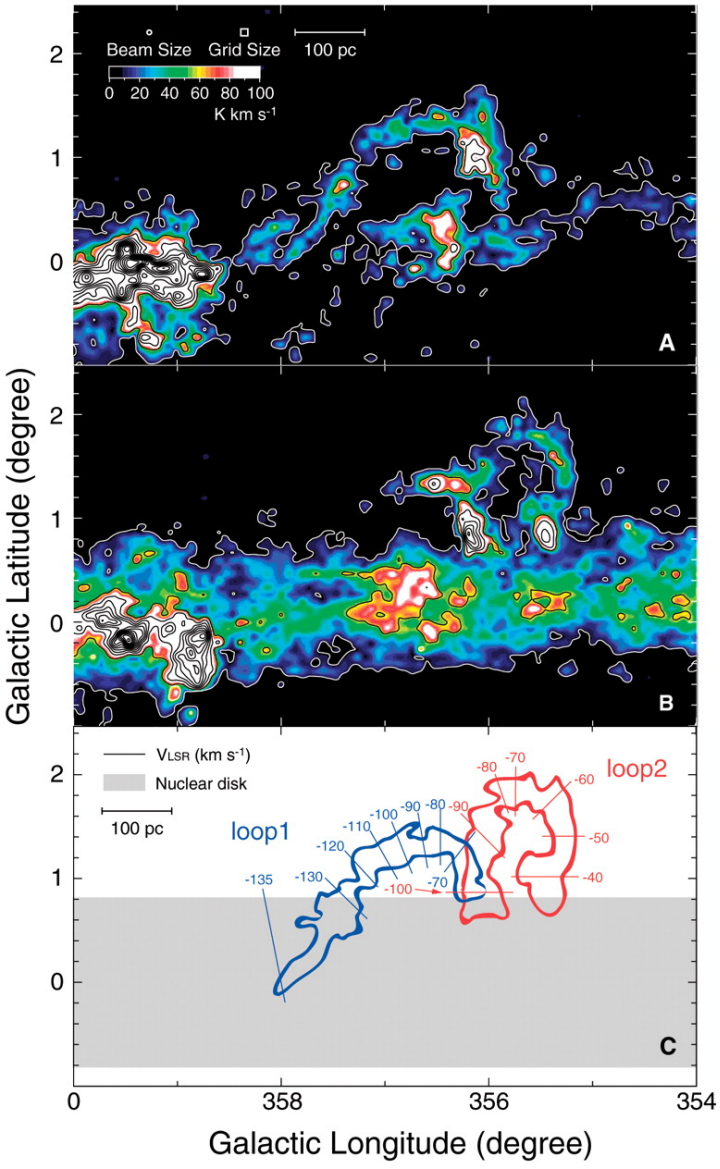

Fukui+ 2006

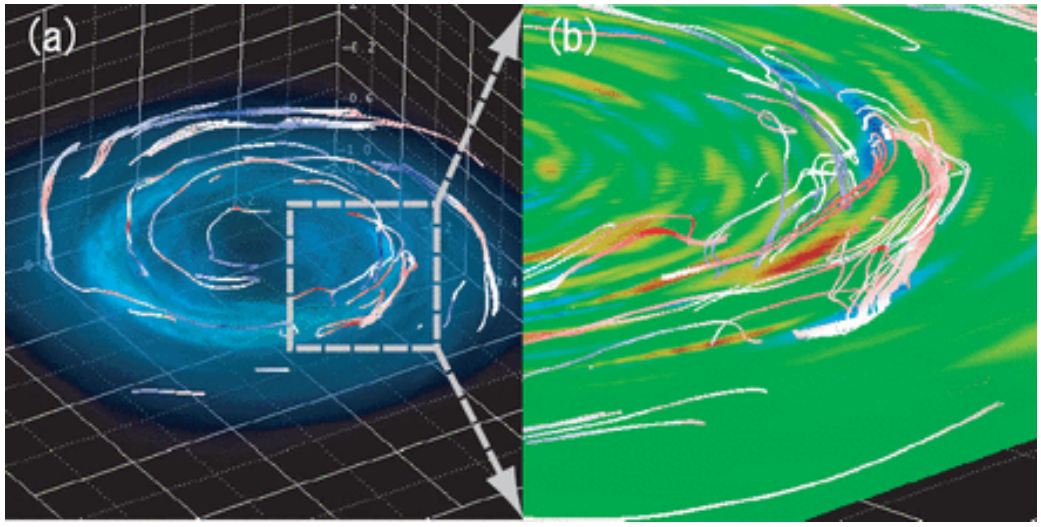

Machida+ 2009

Parker Instability (Mag. Buoyancy)

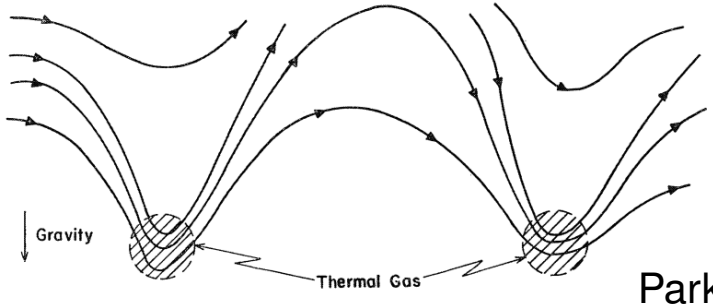

Parker 1966

FIG 2.—Sketch of the local state of the lines of force of the interstellar magnetic field and interstellar gas-cloud configuration resulting from the intrinsic instability of a large-scale field along the galactic disk or arm when confined by the weight of the gas.

B field ⇒ Dynamics

Magnetic Field at Galactic Centre

- $> 50\ \mu$G Crocker+ 2010
  if B is smaller, synchrotron loss is suppressed

  $\Rightarrow$ Overproduce γ–rays by inverse Compton > EGRET(300MeV)
- Complex structure e.g. filaments ~ mG (?)
  Yusef-Zadeh+ 1984; Tsuboi+ 1986; Chuss+ 2003; Oka+ 2005;
  Nishiyama+ 2010; .....
- ~ 5 mG in an IR dark cloud Pillai+ 2015

  via Chandrasekhar-Fermi method

Magnetic Field at Galactic Centre

- $> 50\ \mu$G Crocker+ 2010
  if B is smaller, synchrotron loss is suppressed

  $\Rightarrow$ Overproduce γ–rays by inverse Compton > EGRET(300MeV)
- Complex structure e.g. filaments ~ mG (?)
  Yusef-Zadeh+ 1984; Tsuboi+ 1986; Chuss+ 2003; Oka+ 2005; Nishiyama+ 2010; .....
- ~ 5 mG in an IR dark cloud Pillai+ 2015

  via Chandrasekhar-Fermi method

Comparison of Pressure

- Molecular Clouds:
  $P_{\rm g} \sim 10^{-10}{\rm erg/cm^3}\left(\frac{n}{10^4{\rm cm^{-3}}}\right)\left(\frac{T}{100{\rm K}}\right)$
- Turbulence:
  $P_{\rm turb} \sim 10^{-9}{\rm erg/cm^3}\left(\frac{n}{10^3{\rm cm^{-3}}}\right)\left(\frac{\delta v}{10{\rm km/s}}\right)^2$
- Mag.Field: $P_B \sim 4\times10^{-10}{\rm erg/cm^3}\left(\frac{B}{100\mu{\rm G}}\right)^2$

Aim of This Work

Aim of This Work

Magnetic Activity

⇒Non-Circular & Vertical Flows?

by MHD simulations.

Aim of This Work

Magnetic Activity

⇒Non-Circular & Vertical Flows?

by MHD simulations.

- Axisymmetric potential(Miyamoto & Nagai 1975)

$$\Phi(R,z) = \sum_{i=1}^{3} \frac{-GM_i}{\sqrt{R^2+(a_i+\sqrt{b_i^2+z^2})^2}}$$

	$M_i(10^{10}M_\odot)$	a_i(kpc)	b_i(kpc)
SMBH 1	4.4×10^{-4}	0	0
Bulge 2	2.05	0	0.495
Disk 3	25.47	7.258	0.52

Aim of This Work

Magnetic Activity

⇒Non-Circular & Vertical Flows?

by MHD simulations.

- Axisymmetric potential(Miyamoto & Nagai 1975)

$$\Phi(R,z) = \sum_{i=1}^{3} \frac{-GM_i}{\sqrt{R^2+(a_i+\sqrt{b_i^2+z^2})^2}}$$

	$M_i(10^{10}M_\odot)$	a_i(kpc)	b_i(kpc)
SMBH 1	4.4×10^{-4}	0	0
Bulge 2	2.05	0	0.495
Disk 3	25.47	7.258	0.52

- Study the gas dynamics under the fixed grav. potential.

MHD Simulation –Setup–

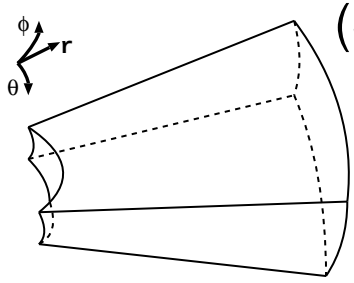

(Suzuki & Inutsuka 2009; 2014 for Protoplanetaray Disks)

- Simulation Region (3D Spherical Coordinates): $(r, \theta, \phi) = (0.01 - 60\ \mathrm{kpc}, \pm\pi/3, 2\pi)$ (full rot.) resolved by (384,128,256)

- Ideal MHD Equations (Newtonian)

  Mass consv.: $\frac{\partial \rho}{\partial t} + \nabla \cdot (\rho v) = 0$

  Mom. consv.: $\frac{dv}{dt} + \frac{1}{\rho}\nabla\left(p + \frac{B^2}{8\pi}\right) - \frac{(B\cdot\nabla)B}{4\pi\rho} + \nabla\Phi = 0$

  Eng. consv.: $\rho\frac{de}{dt} = -p\nabla \cdot v$

  B evol.: $\frac{\partial B}{\partial t} = \nabla \times (v \times B)$ with $\nabla \cdot B = 0$

- Locally Isothermal

- Initial Mag. field: $B_z = 0.71\mu\mathrm{G}\left(\frac{R}{1\ \mathrm{kpc}}\right)^{-1}$ in $R > 35$ pc

Overview

▸ 2kpc-long ▸ 2kpc-short ▸ 1kpc-long ▸ 1kpc-short ▸ 0.6kpc-short

Amplification of Magnetic Field

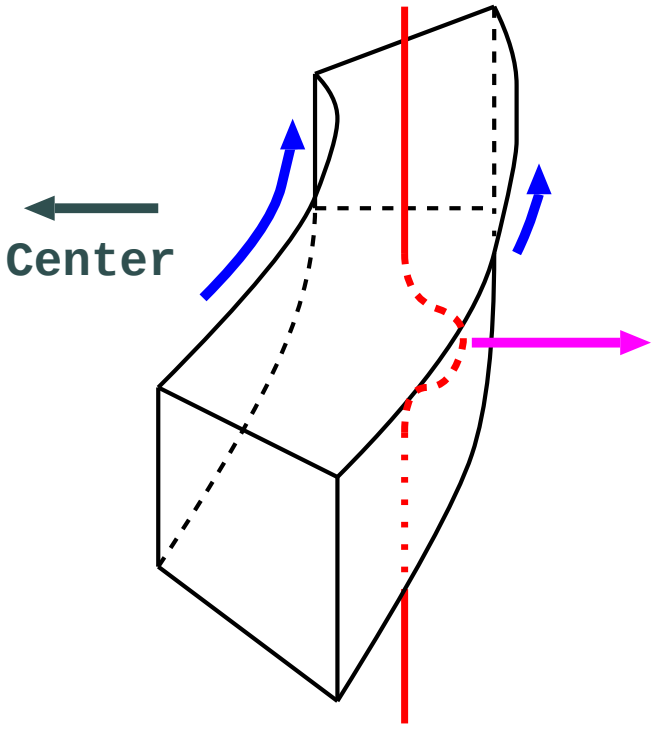

Magneto-Rotational Instability

(Velikhov 1959; Chandrasekhar 1961; Balbus & Hawley 1991)

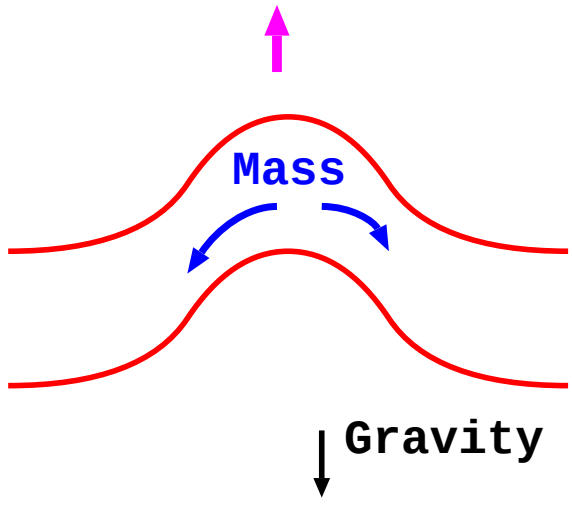

Parker Instability (Magnetic Buoyancy)

(Parker 1966)

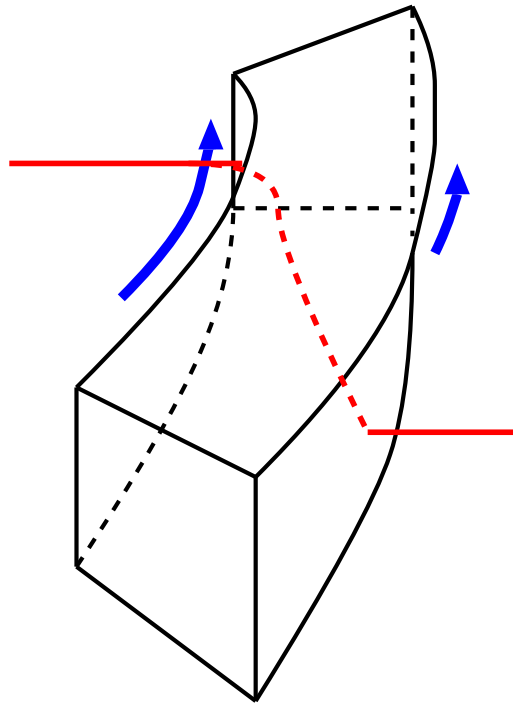

B_ϕ Generation by Differential Rotation

▸ Stratified MRI ▸ Local MRI

Evolution of B

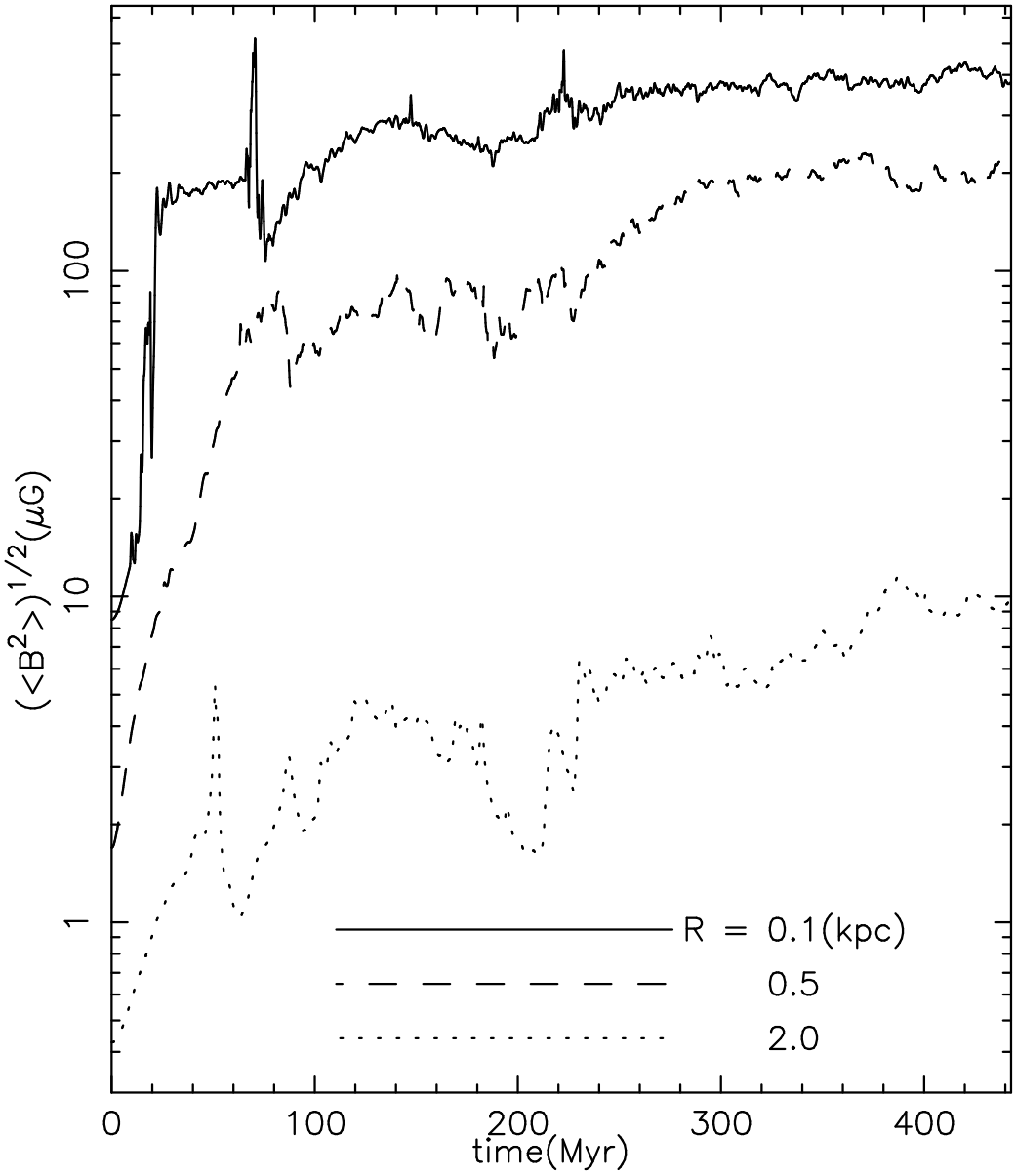

ϕ (azimuthal) & z (vertical) averaged

Average B

- 400-500μG at 0.1 kpc
- 200μG at 0.5 kpc

Face-on View (@Galactic Plane)

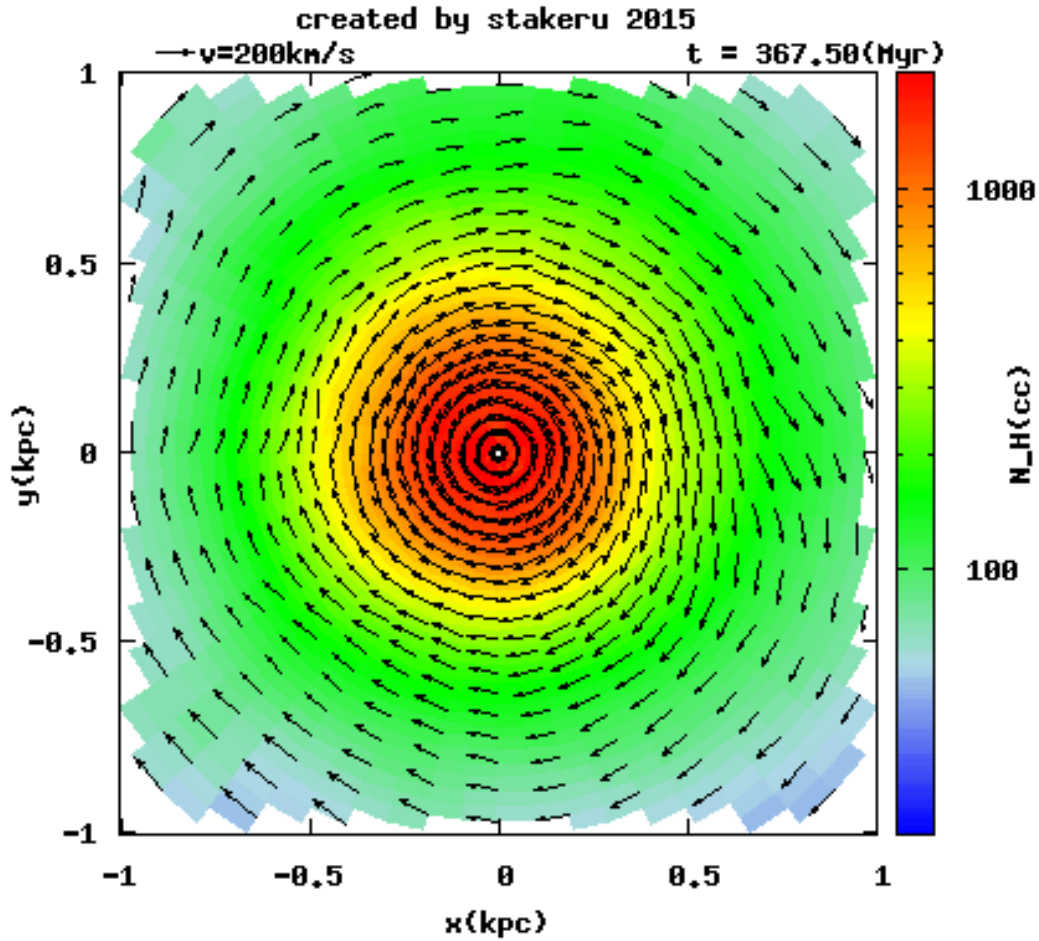

l–v diagram near GC

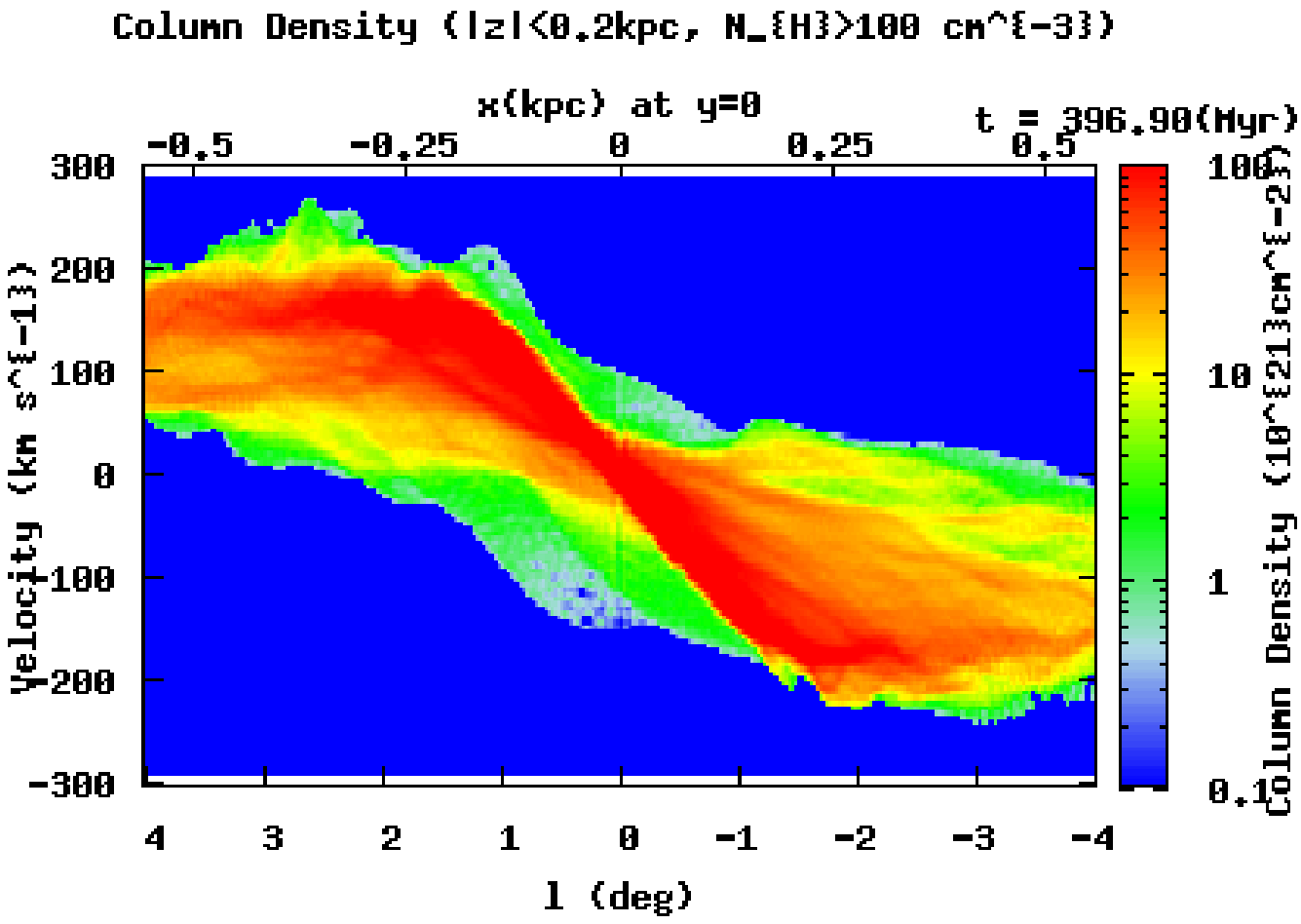

(Only $N_{\mathrm{H}} > 100$ cm^{-3} used to derive Column density)

l–v diagram near GC

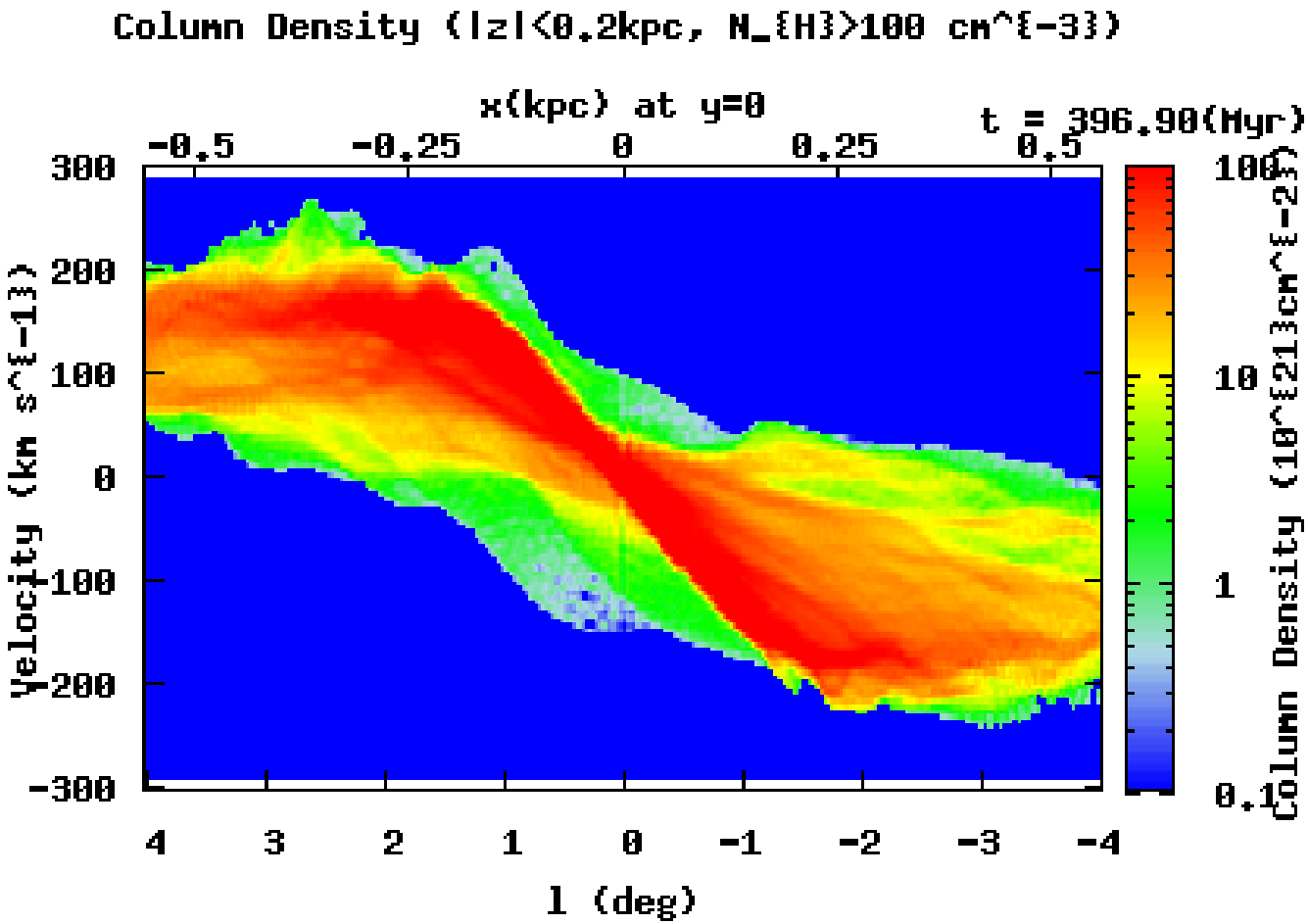

(Only $N_{\mathrm{H}} > 100$ cm^{-3} used to derive Column density)

Time-dependent Parallelogram

l–v diagram: Observation – Simulation

l–*v* diagram: Observation – Simulation

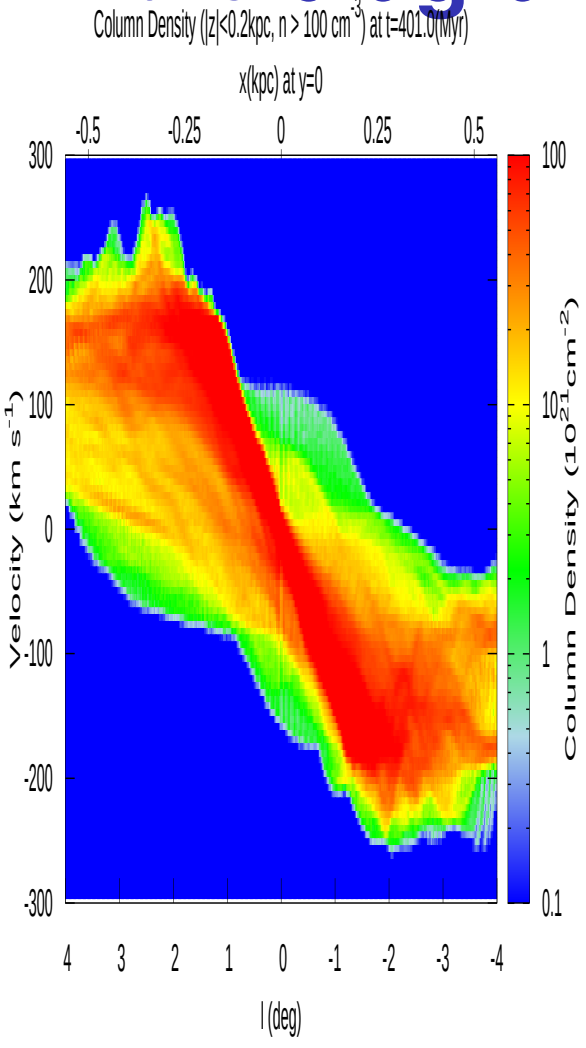

l–v diagram: Observation – Simulation

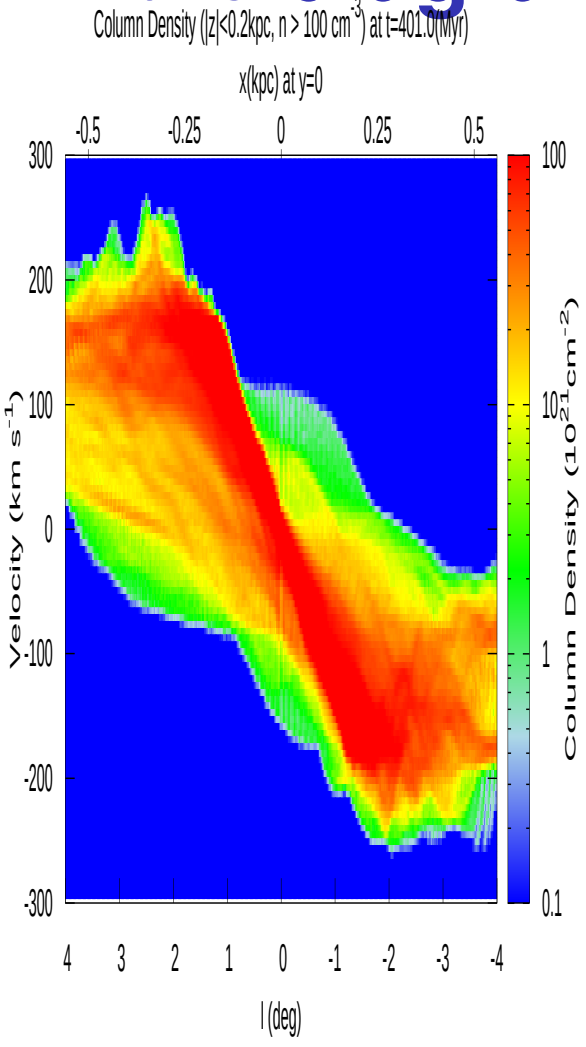

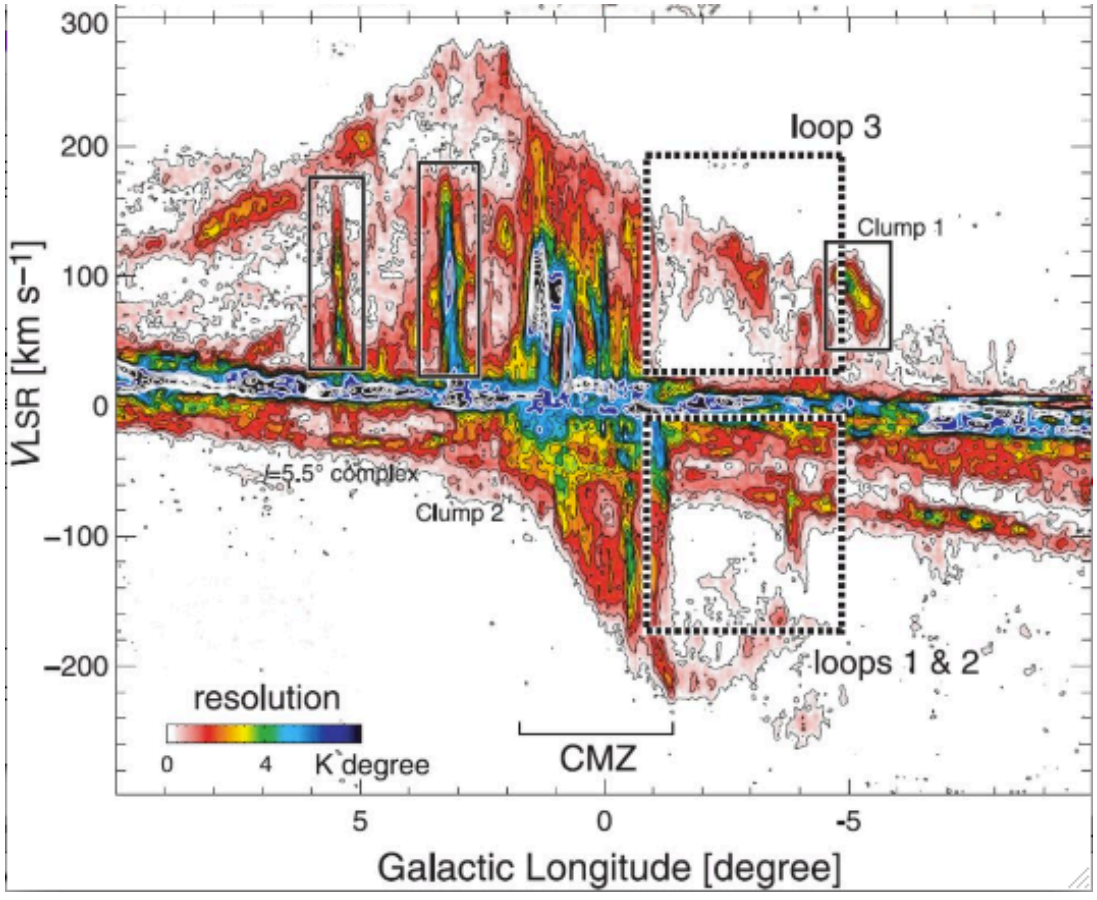

NANTEN Obs. Torii+ 2010

Need $N(H_2)/I(CO)(\approx 2.3\times10^{20}\mathrm{cm}^{-2}(\mathrm{K\ km\ s}^{-1})^{-1})$ (Strong+ 1988)

for direct comparison

l–v diagram: B-field vs. Bar Potential

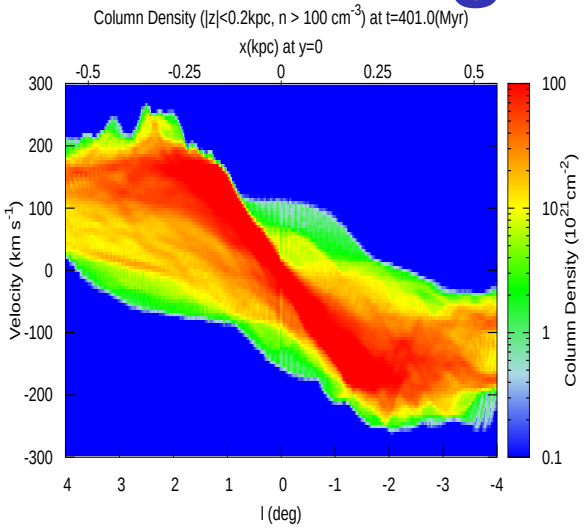

Our Result

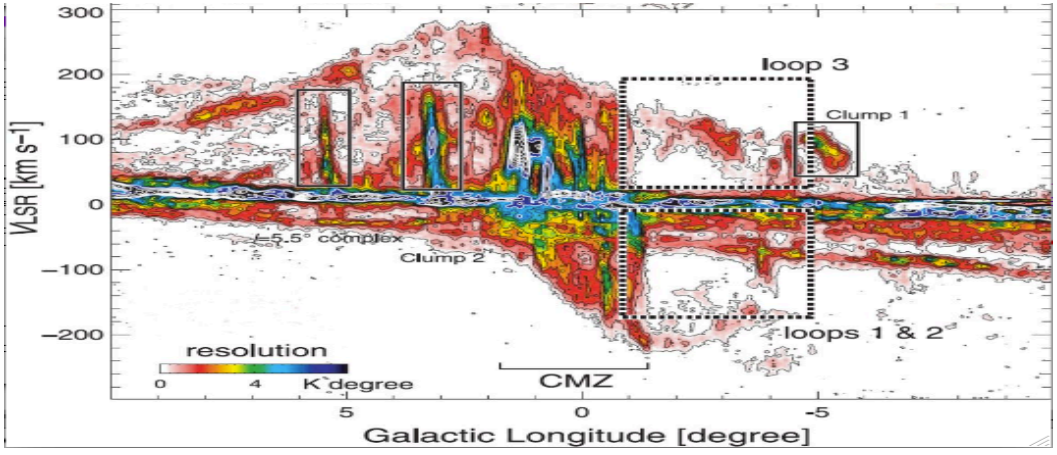

NANTEN Obs. Torii+ 2010

l–v diagram: B-field vs. Bar Potential

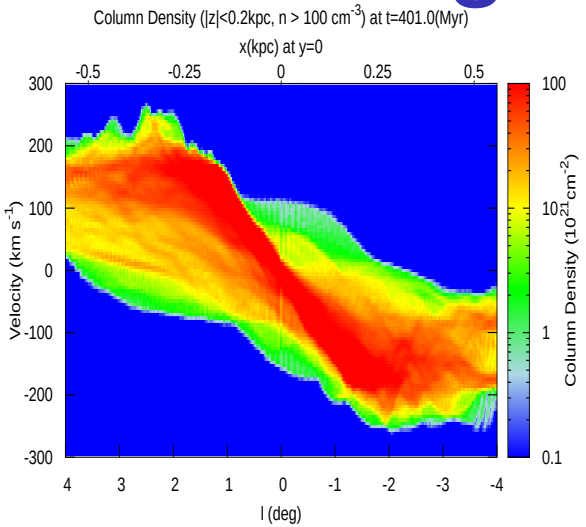

Our Result

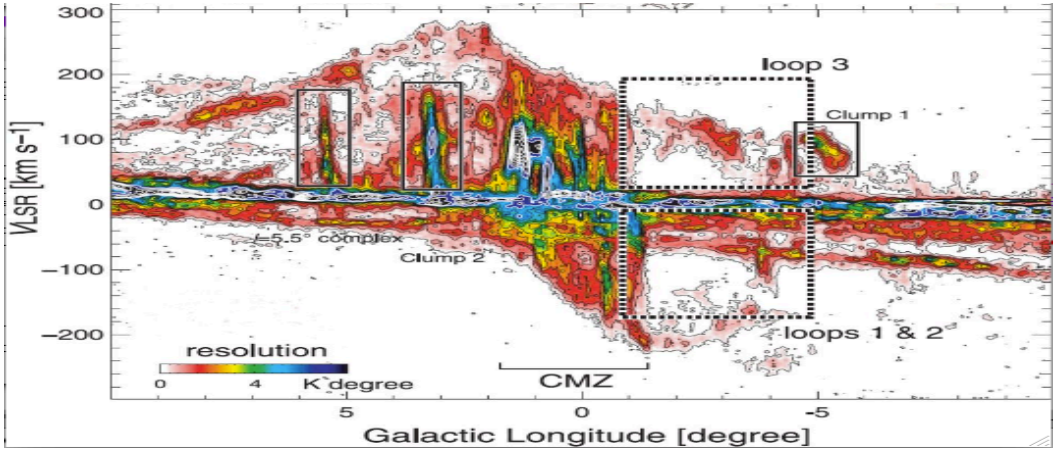

NANTEN Obs. Torii+ 2010

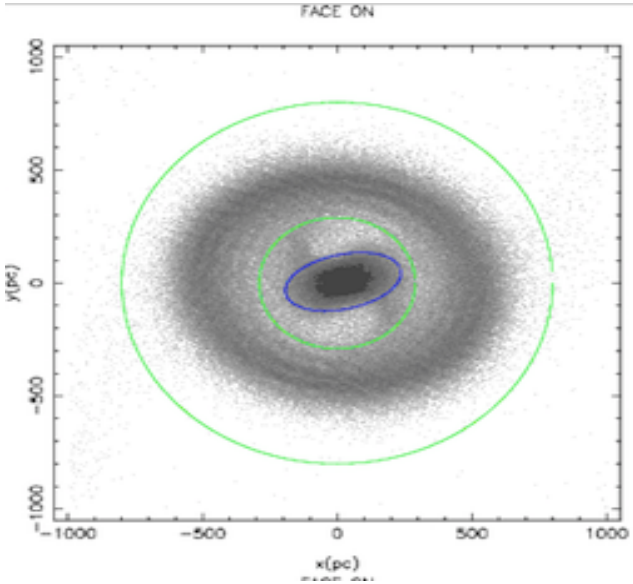

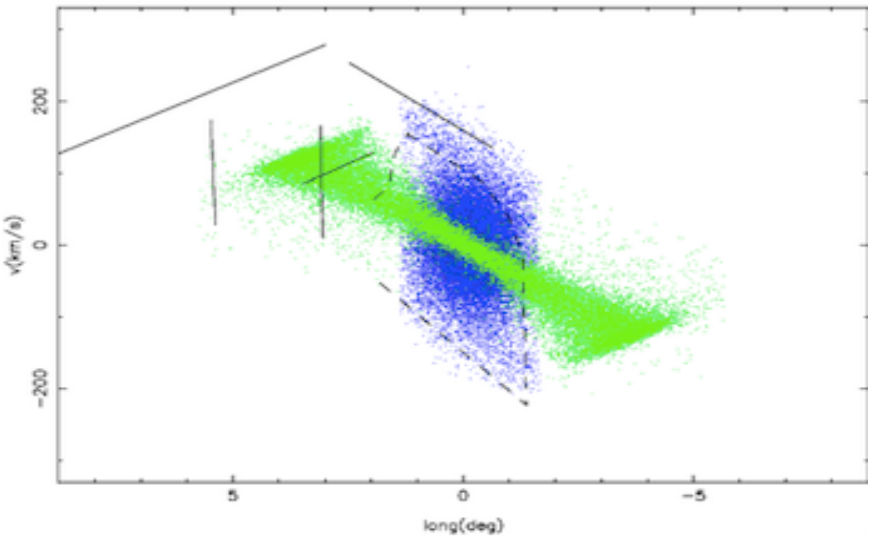

with Bar Potential & Hydro (Rodriguez-Fernandez & Combes 2008)

Excitation of Non-circular Motion

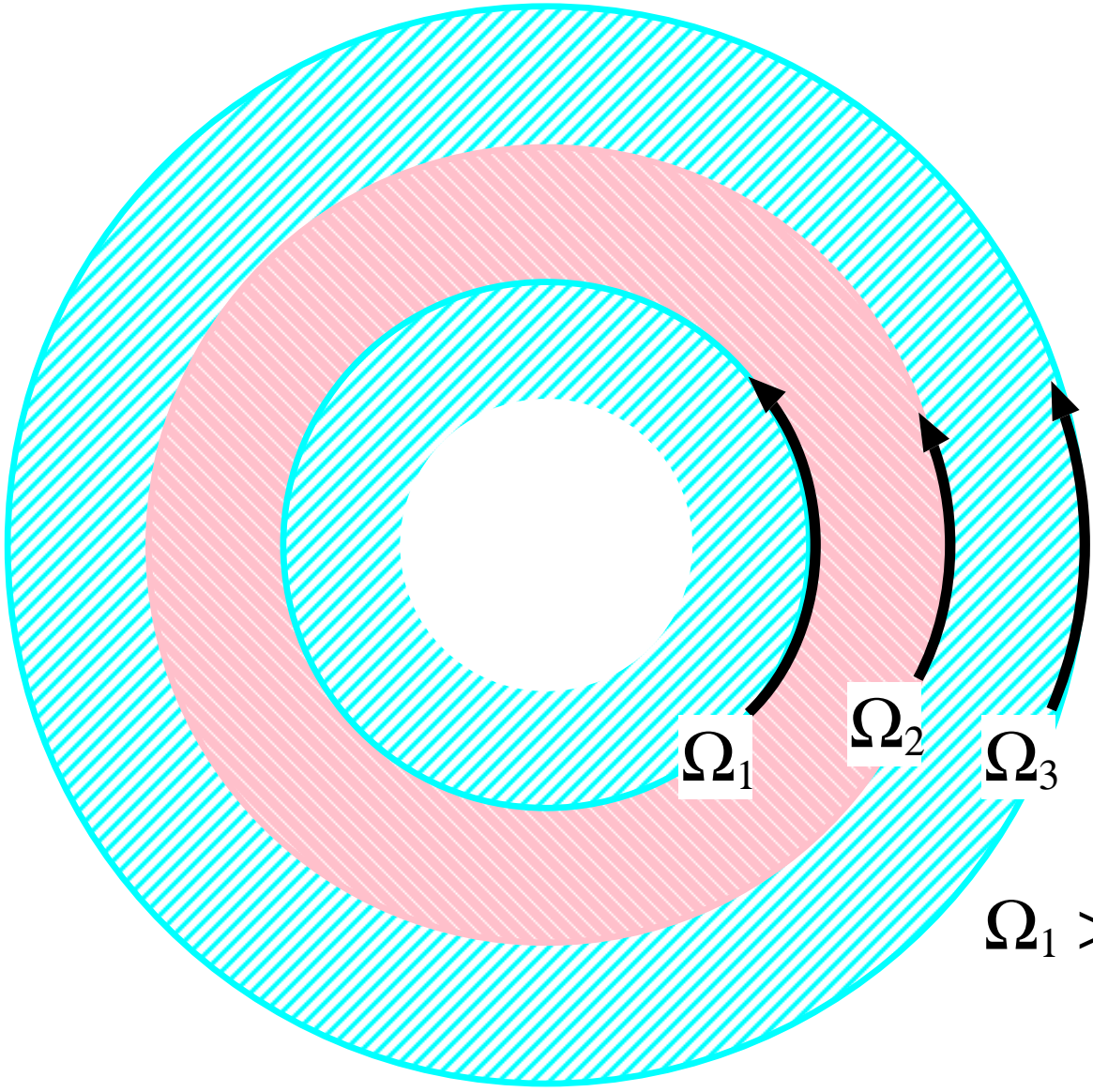

$$\Omega_1 > \Omega_2 = \Omega_3$$

Amplification of Magnetic Field

Amplification of Magnetic Field

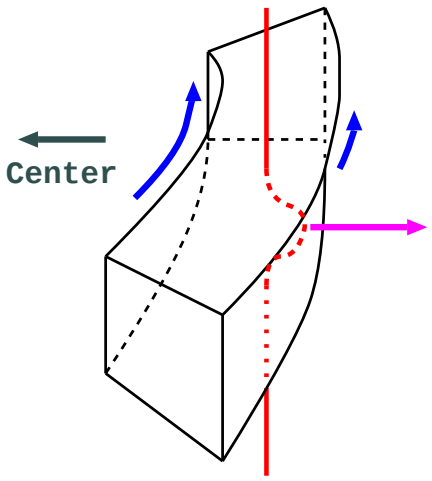

MagnetoRotational Instability

- Growth Rate of MRI

$$\frac{\omega_{\mathrm{MRI,max}}}{\Omega} = \frac{1}{2}\left|\frac{\partial \ln \Omega}{\partial \ln R}\right|$$

$\omega_{\mathrm{MRI,max}}$ for most unstable mode

Amplification of Magnetic Field

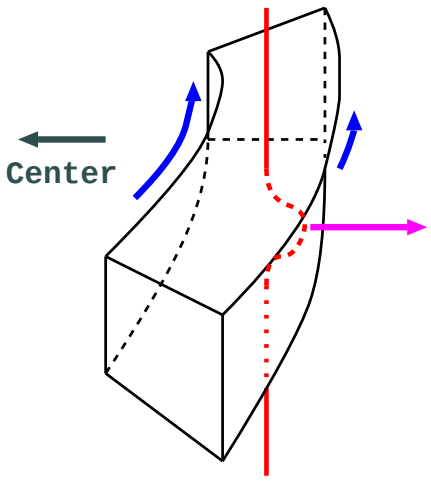

MagnetoRotational Instability

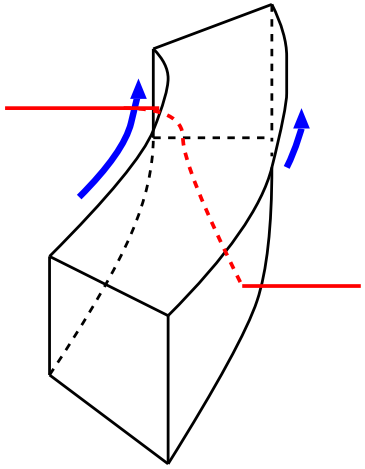

B_ϕ Generation by Differential Rotation

- Growth Rate of MRI

$$\frac{\omega_{\mathrm{MRI,max}}}{\Omega} = \frac{1}{2}\left|\frac{\partial \ln \Omega}{\partial \ln R}\right|$$

$\omega_{\mathrm{MRI,max}}$ for most unstable mode

- Winding by Dif.Rot.

$$\frac{\partial B}{\partial t} = \nabla \times (v \times B)$$

$$\Rightarrow \frac{1}{\Omega}\frac{\partial B_\phi}{\partial t} = B_R \frac{\partial \ln \Omega}{\partial \ln R}$$

Amplification of Magnetic Field

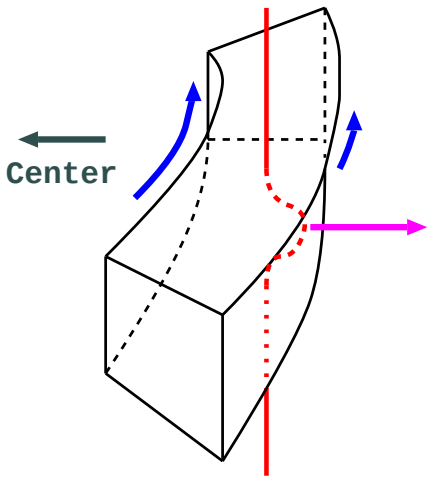

MagnetoRotational Instability

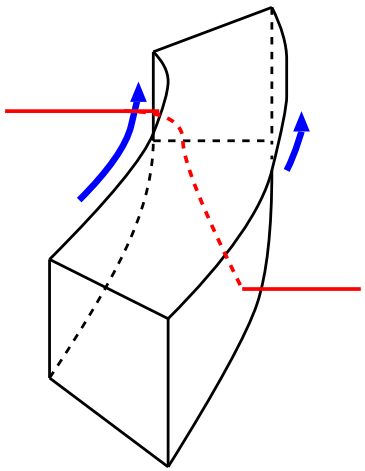

B_ϕ Generation by Differential Rotation

- Growth Rate of MRI

$$\frac{\omega_{\mathrm{MRI,max}}}{\Omega} = \frac{1}{2}\left|\frac{\partial \ln \Omega}{\partial \ln R}\right|$$

$\omega_{\mathrm{MRI,max}}$ for most unstable mode

- Winding by Dif.Rot.

$$\frac{\partial B}{\partial t} = \nabla \times (v \times B)$$

$$\Rightarrow \frac{1}{\Omega}\frac{\partial B_\phi}{\partial t} = B_R \frac{\partial \ln \Omega}{\partial \ln R}$$

Strong Dif.Rot. (large $\left|\frac{\partial \ln \Omega}{\partial \ln R}\right|$)

$\Rightarrow$ Fast Amplification of B

- Strong B field
- Efficient Transport of Angular Momentum (large α)

Excitation of Non-circular Motion

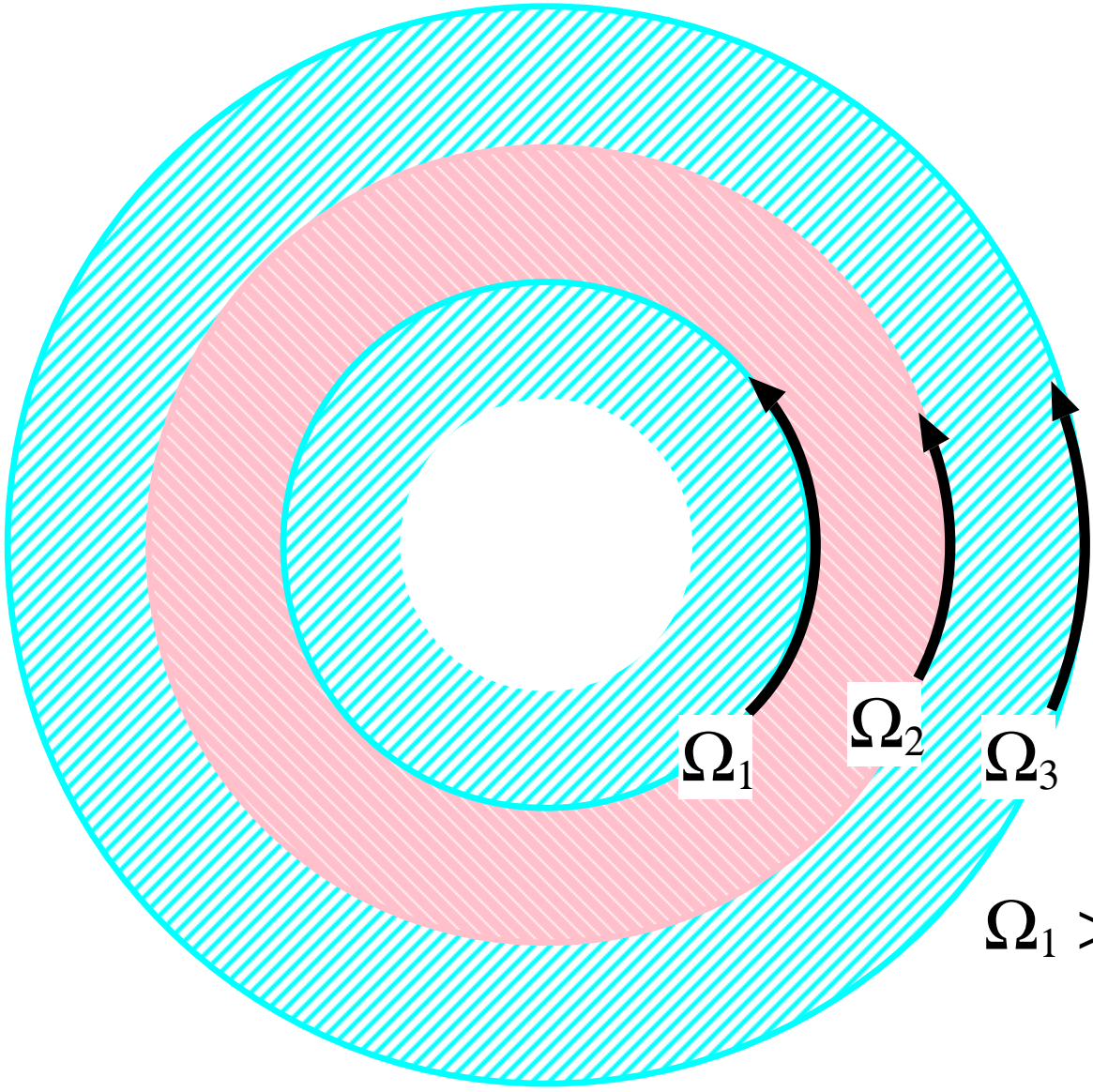

$$\Omega_1 > \Omega_2 = \Omega_3$$

Excitation of Non-circular Motion

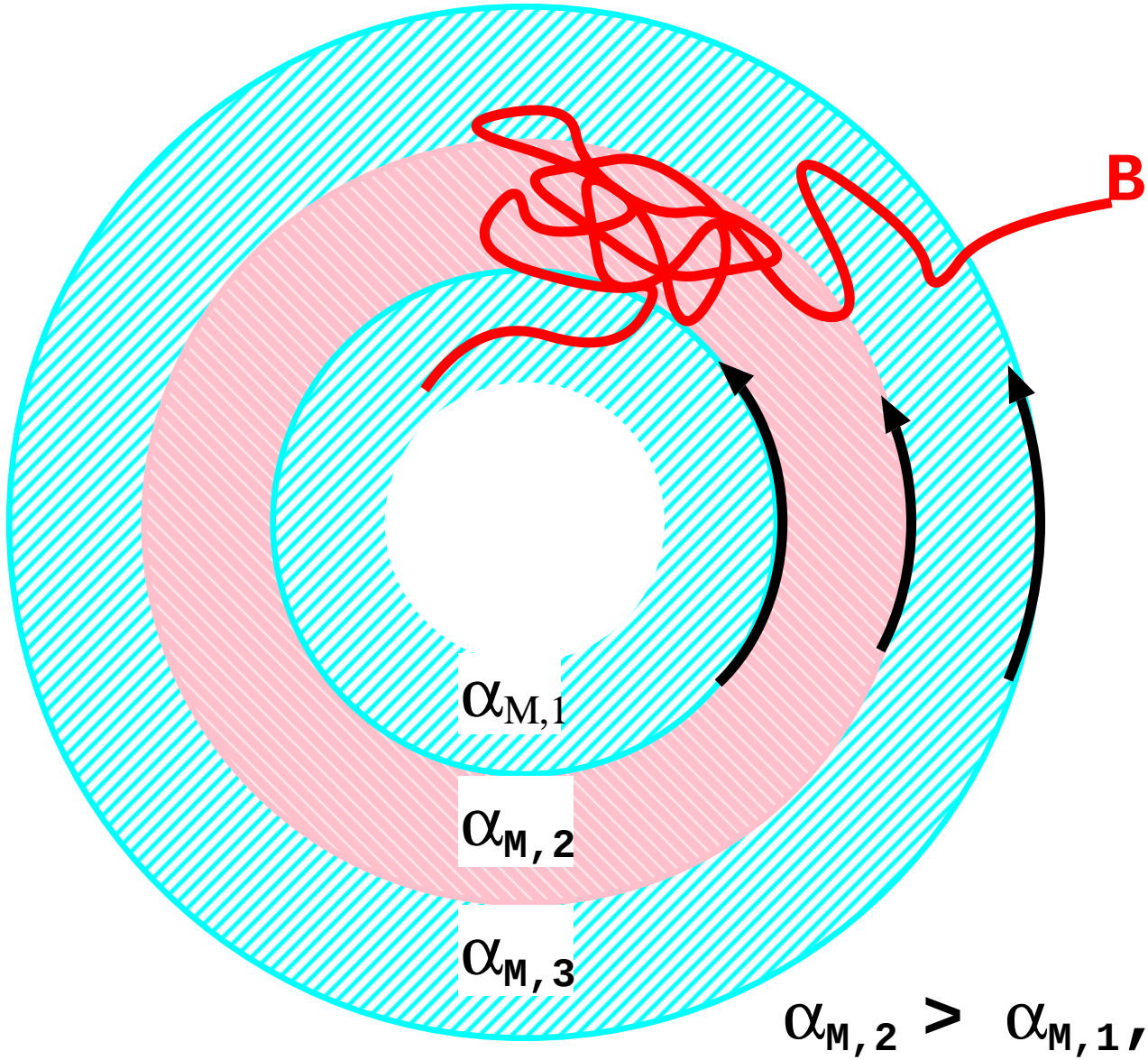

$\alpha_{M,2} > \alpha_{M,1}, \alpha_{M,3}$

Excitation of Non-circular Motion

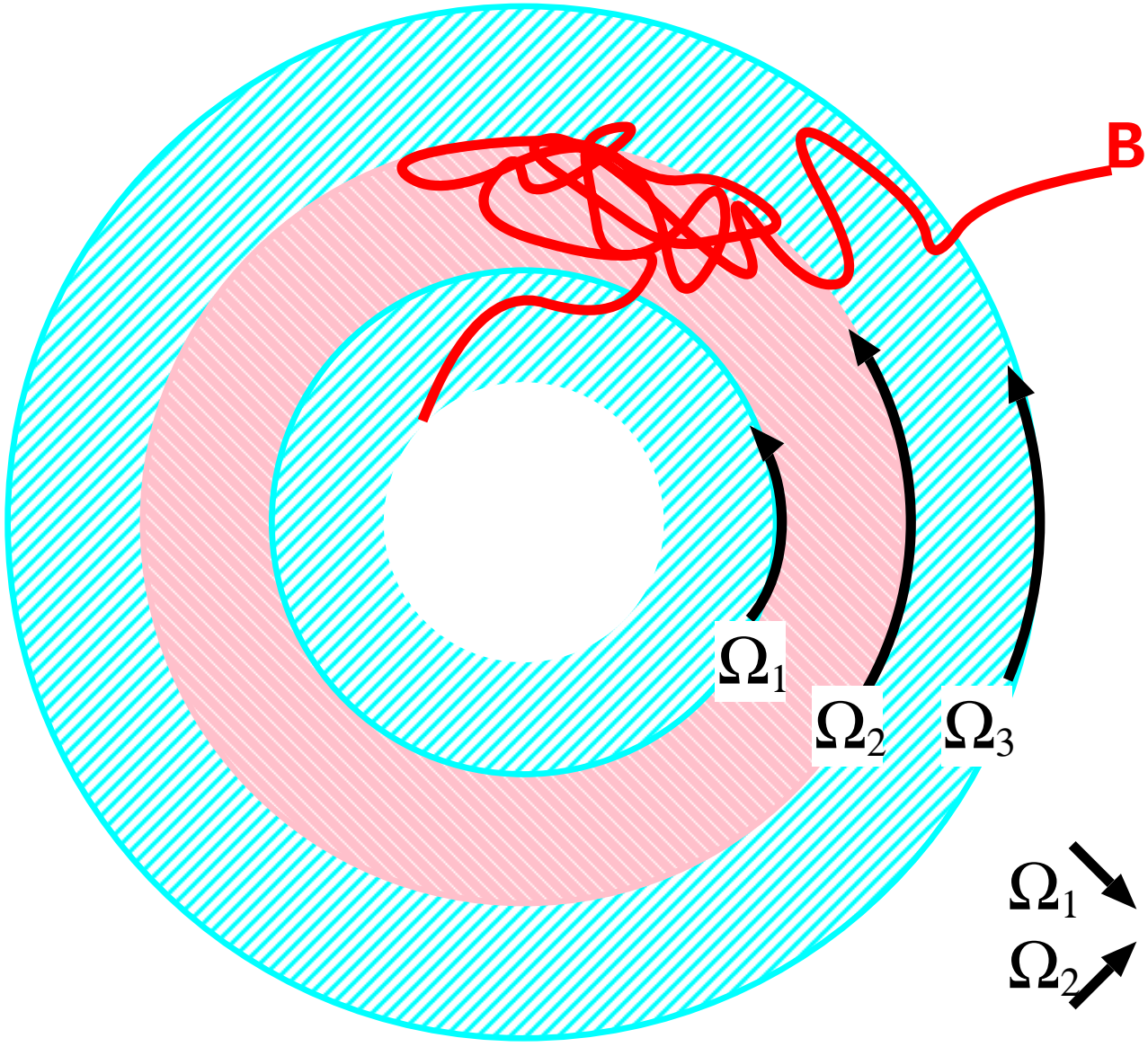

Excitation of Non-circular Motion

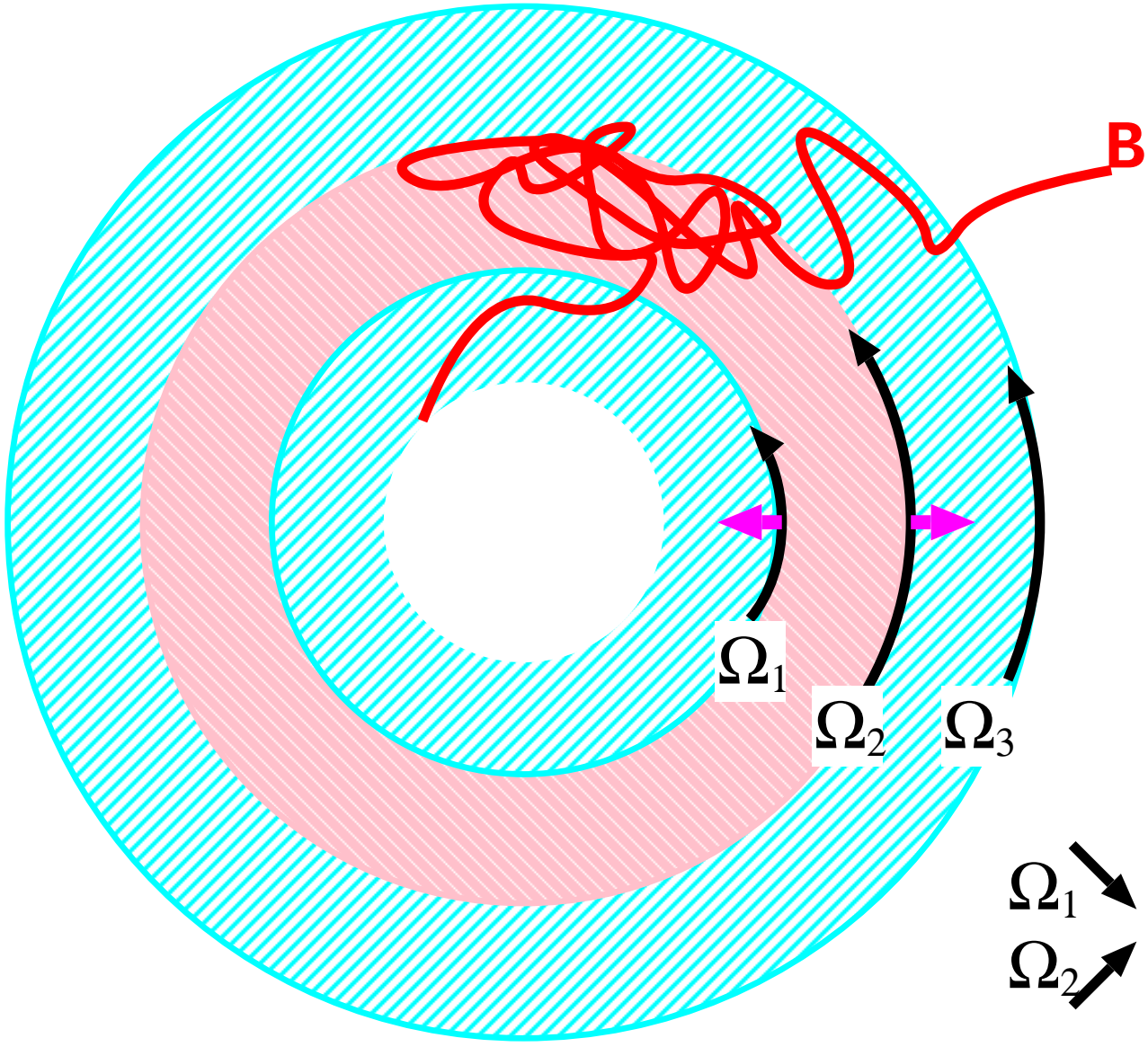

Outflows

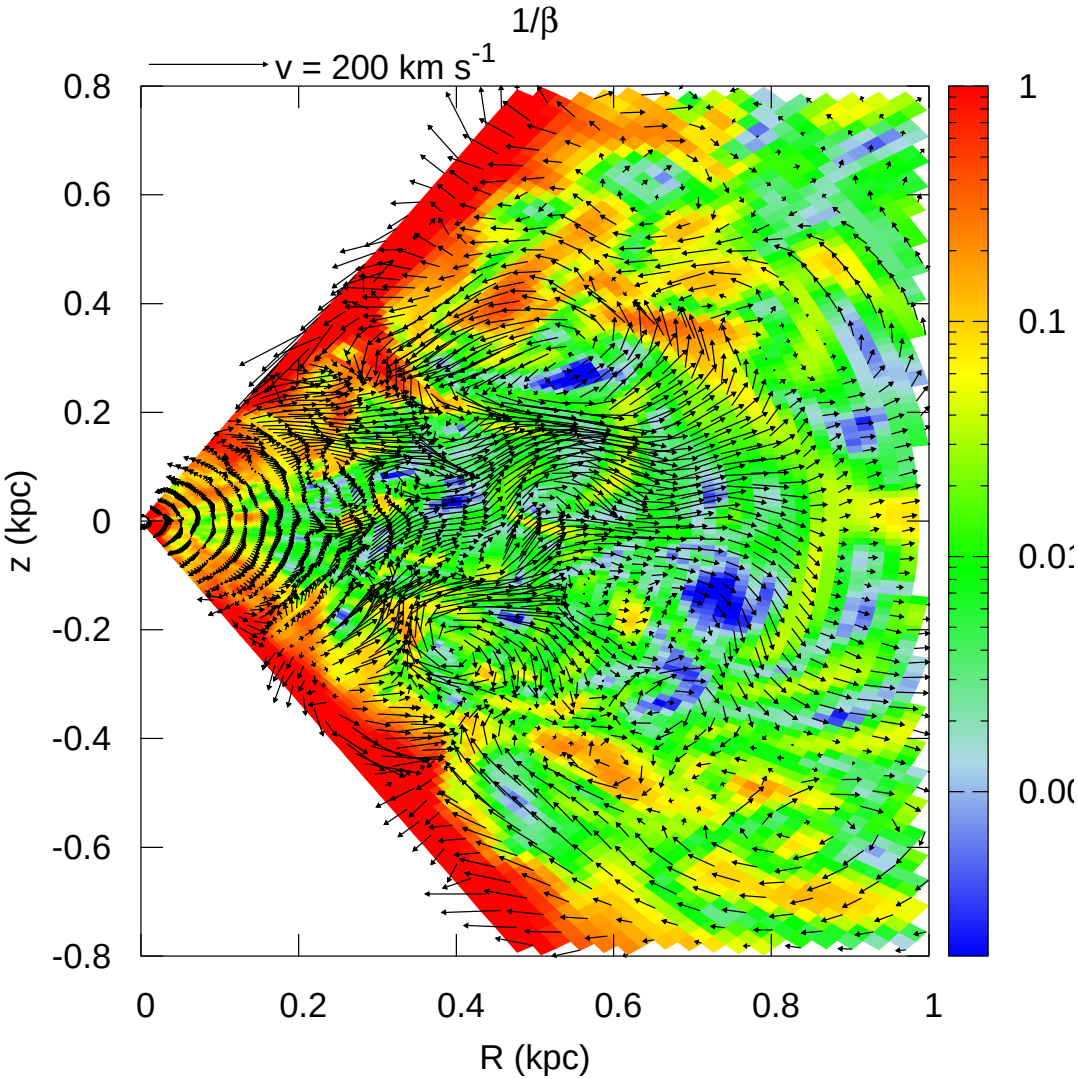
1/β
v = 200 km s-1
0.8
0.6
0.4
0.2
0
-0.2
-0.4
-0.6
-0.8
z (kpc)
0
0.2
0.4
0.6
0.8
1
R (kpc)
1
0.1
0.0

Outflows

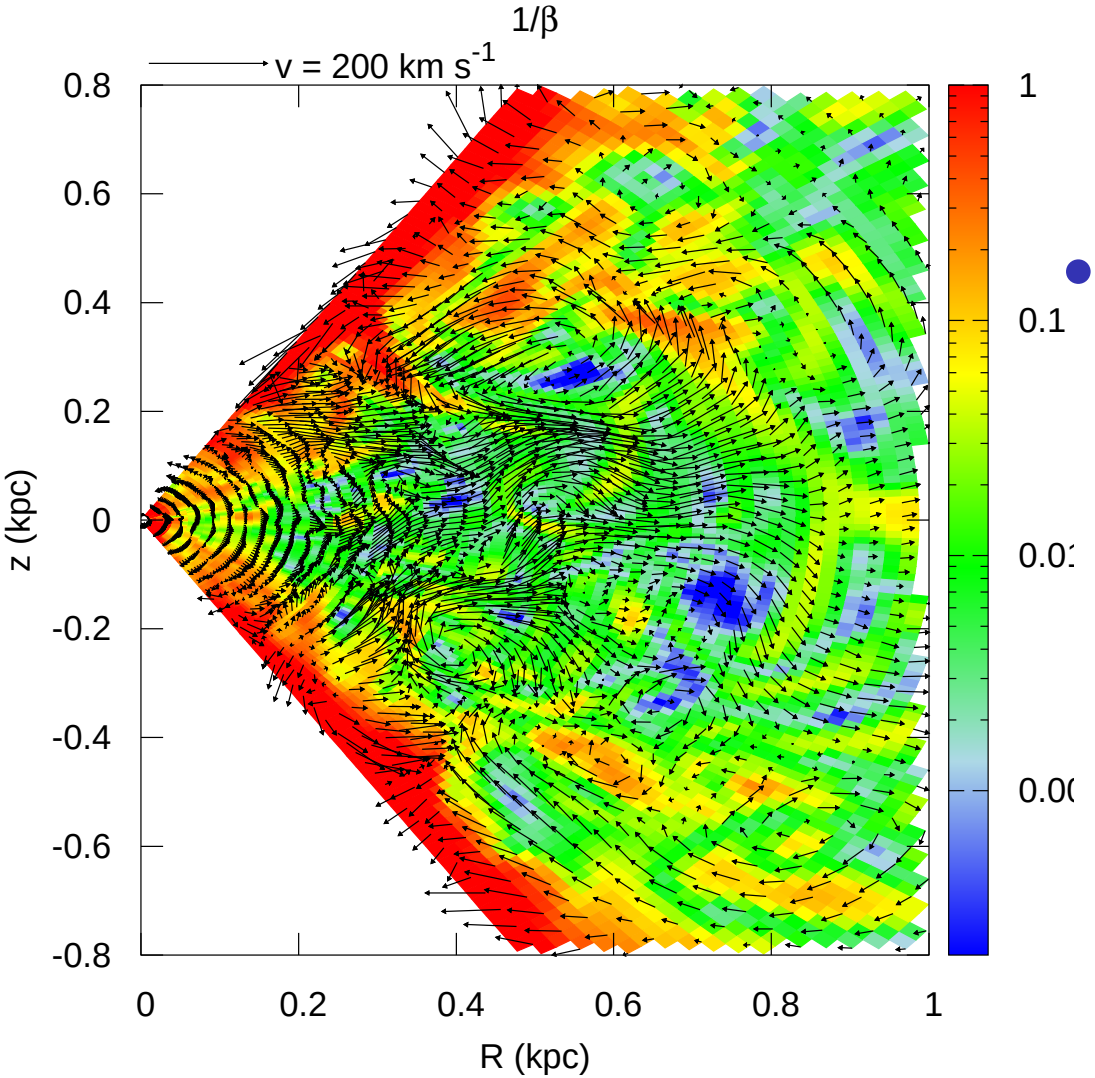

- Mass outflow rate:
  $\dot{M} \approx 70 M_{\odot}/\mathrm{yr}$

Outflows

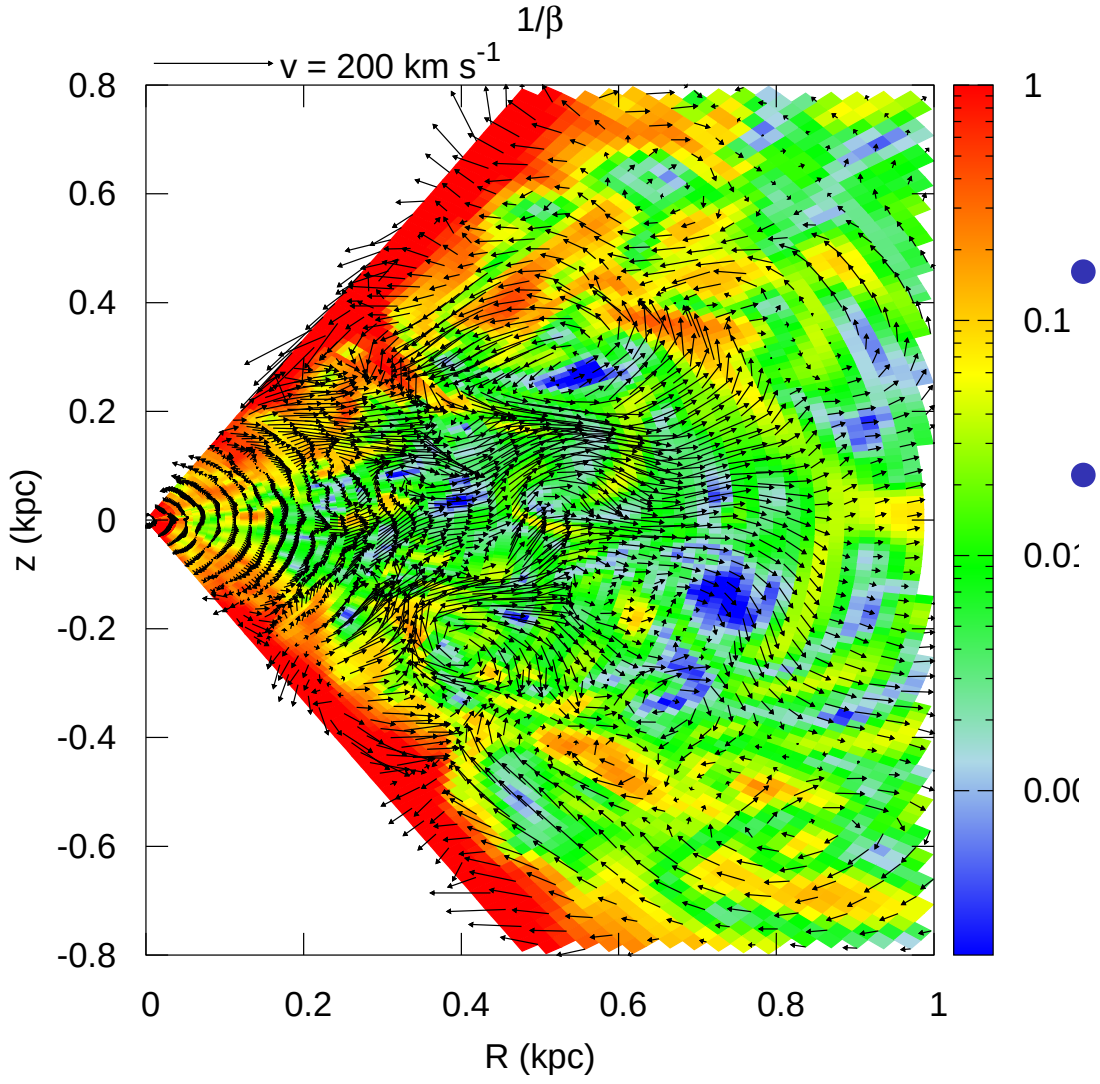

- Mass outflow rate: $\dot{M} \approx 70 M_{\odot}/\mathrm{yr}$
- Kinetic Luminosity: $\frac{1}{2}\dot{M}v \approx$ $10^{41}\left(\frac{v}{50\mathrm{km/s}}\right)^2 \mathrm{erg/s}$ $\approx 3\times10^{48}\mathrm{erg/yr}$

Fermi Bubble

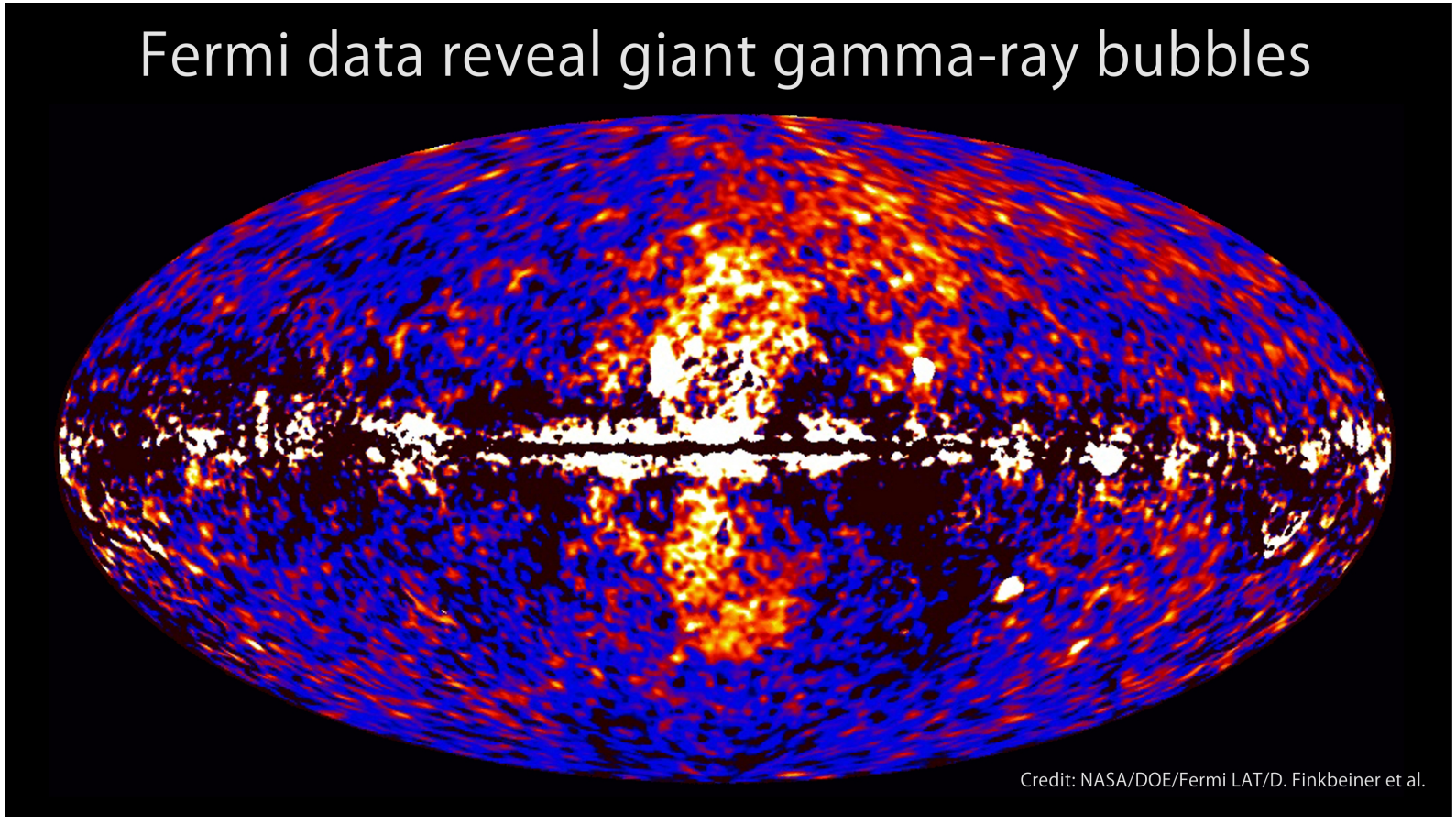

Fermi Bubble

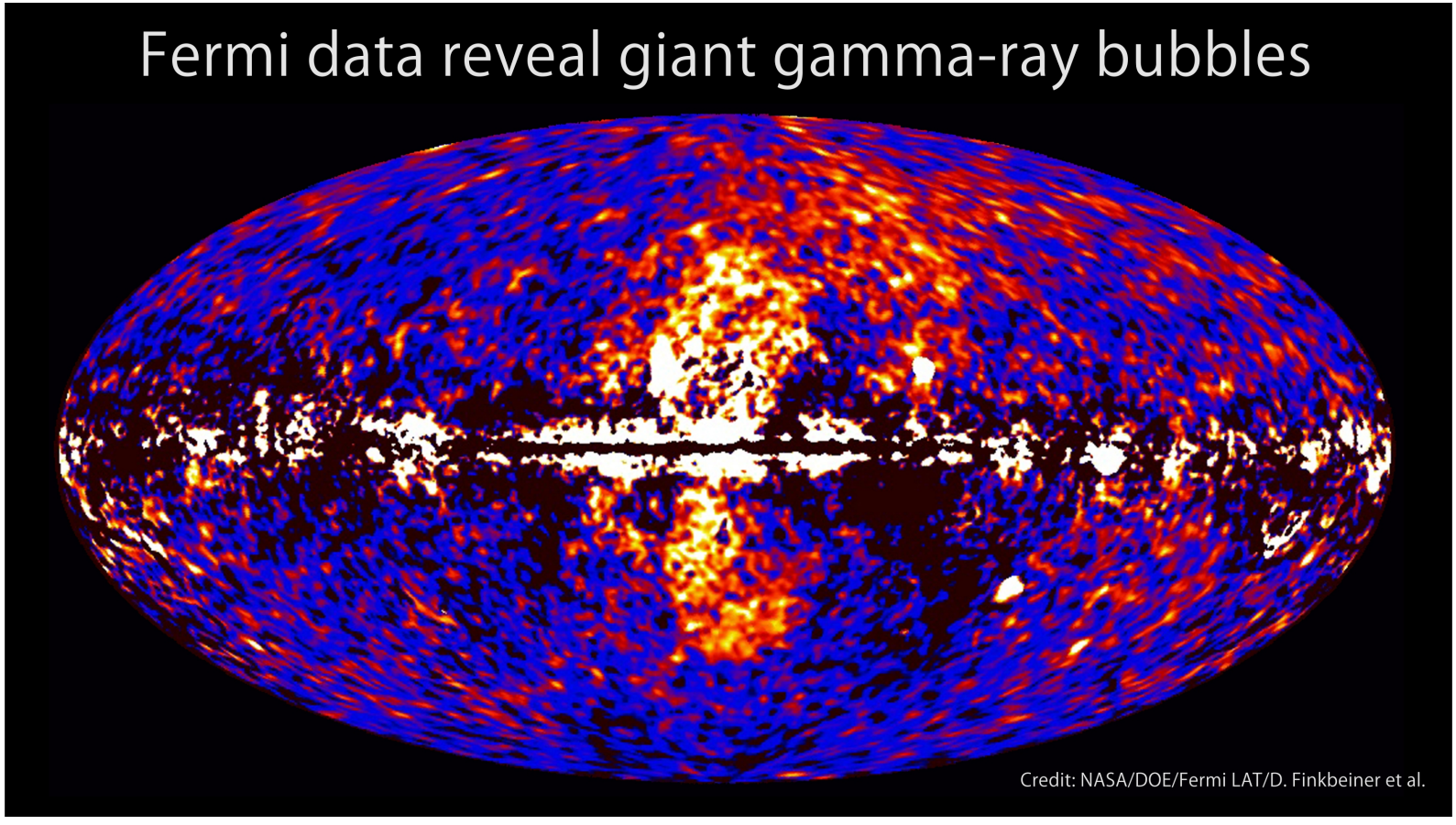

- Energetics from X-ray obs

  $n \sim 10^{-2}\mathrm{cm}^{-3}$, $kT \sim 2\mathrm{keV}$, $l \sim 10\mathrm{kpc}$

  $\Rightarrow E \sim 10^{54-55}\mathrm{erg}$

Fermi Bubble

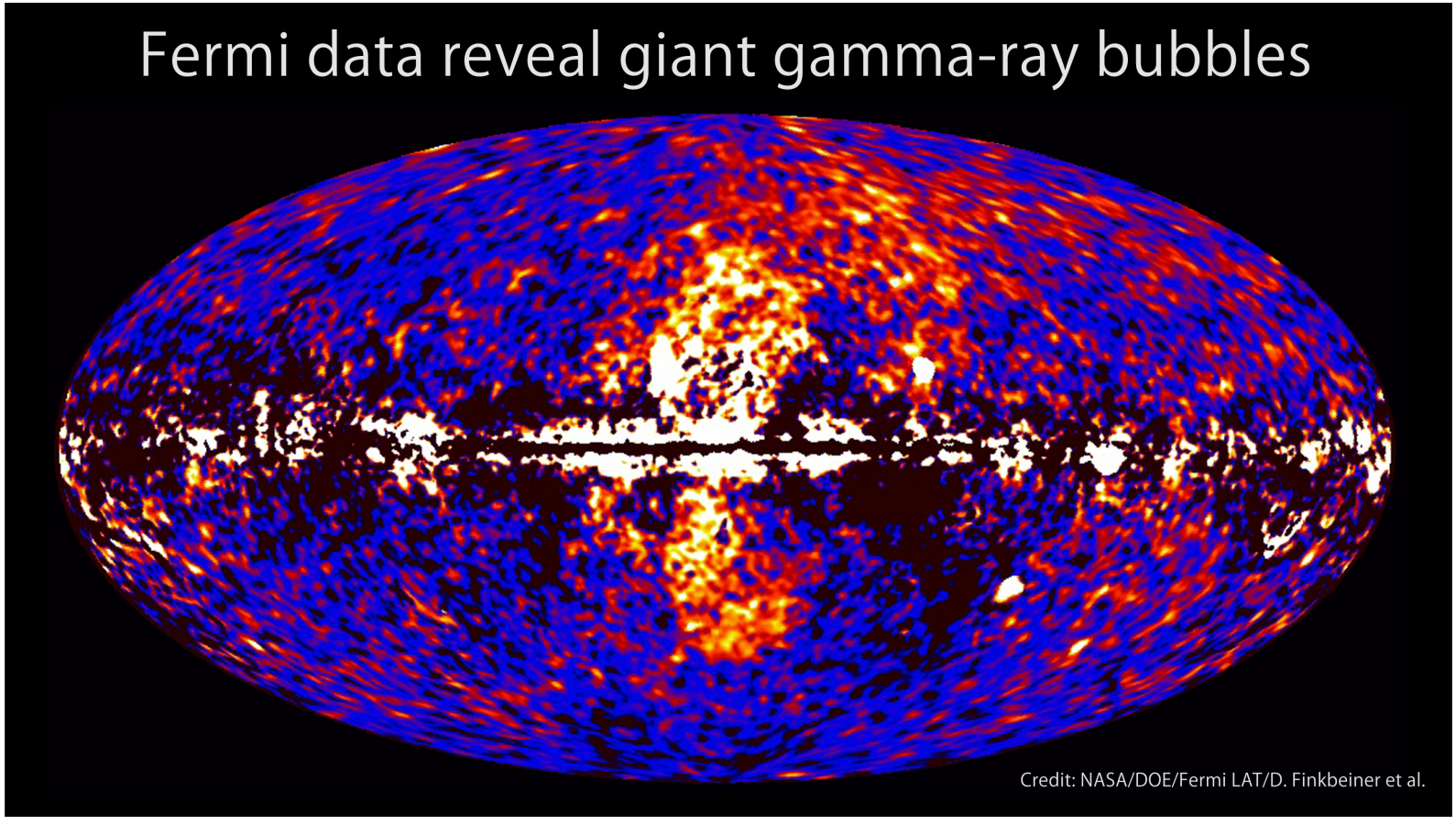

- Energetics from X-ray obs
  $n \sim 10^{-2}\mathrm{cm}^{-3}$, $kT \sim 2\mathrm{keV}$, $l \sim 10\mathrm{kpc}$
  $\Rightarrow E \sim 10^{54-55}\mathrm{erg}$
- Required $v \sim 10^{2-3}\mathrm{km/s} \Rightarrow \tau \sim 10^{7}\mathrm{yr}$

Fermi Bubble

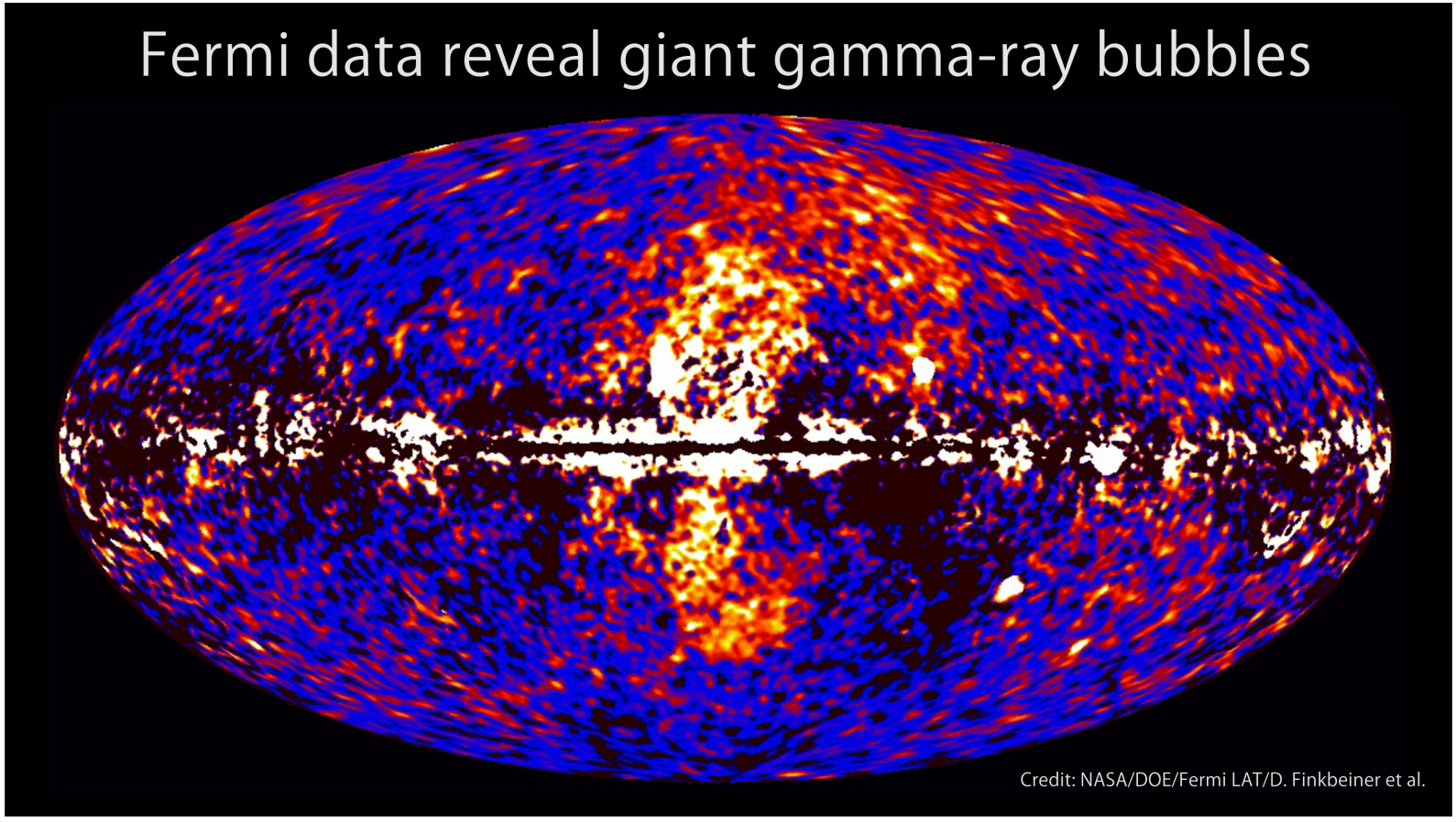

- Energetics from X-ray obs
  $n \sim 10^{-2}\mathrm{cm}^{-3}$, $kT \sim 2\mathrm{keV}$, $l \sim 10\mathrm{kpc}$
  $\Rightarrow E \sim 10^{54-55}\mathrm{erg}$
- Required $v \sim 10^{2-3}\mathrm{km/s} \Rightarrow \tau \sim 10^{7}\mathrm{yr}$

Required Input $E/\tau \sim 10^{48}\mathrm{erg/yr}$

Magnetic Activity – Fermi Bubble ???

Magnetic Activity – Fermi Bubble ???

- Outflow in Simulation: $\approx 3 \times 10^{48}$erg/yr

Magnetic Activity – Fermi Bubble ???

- Outflow in Simulation: $\approx 3 \times 10^{48}$erg/yr
- Required Input for Fermi Bubble: $\sim 10^{48}$erg/yr

Magnetic Activity – Fermi Bubble ???

- Outflow in Simulation: $\approx 3 \times 10^{48}$erg/yr
- Required Input for Fermi Bubble: $\sim 10^{48}$erg/yr

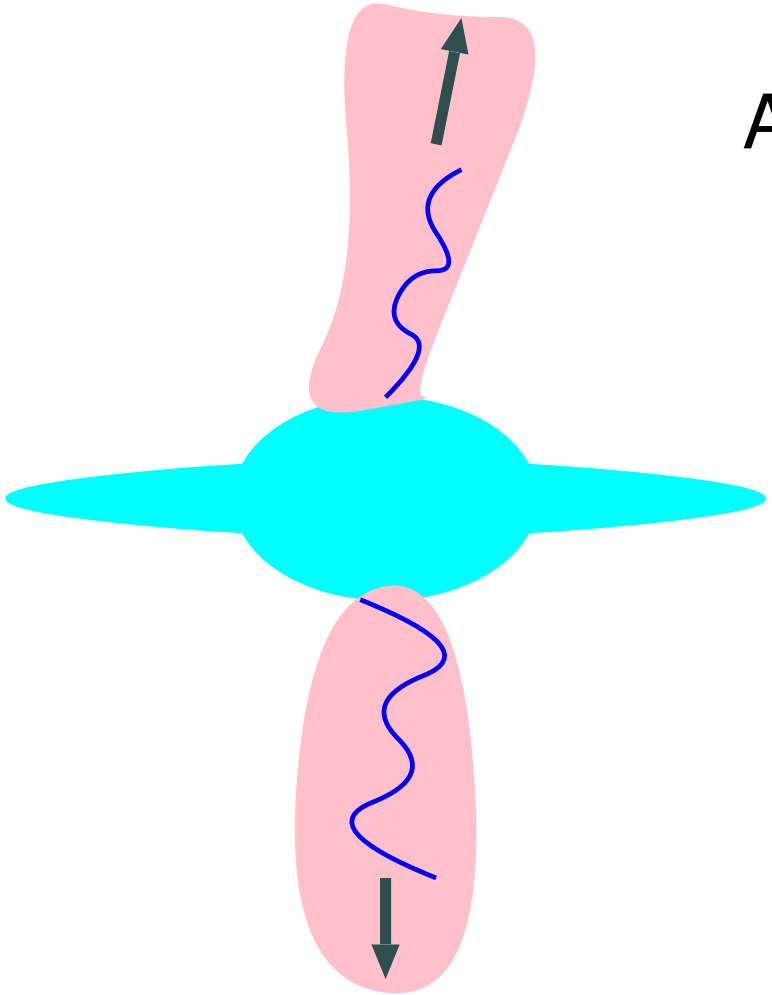

Alfvén wave emission

Magnetic Activity – Fermi Bubble ???

- Outflow in Simulation: $\approx 3\times10^{48}$erg/yr
- Required Input for Fermi Bubble: $\sim 10^{48}$erg/yr

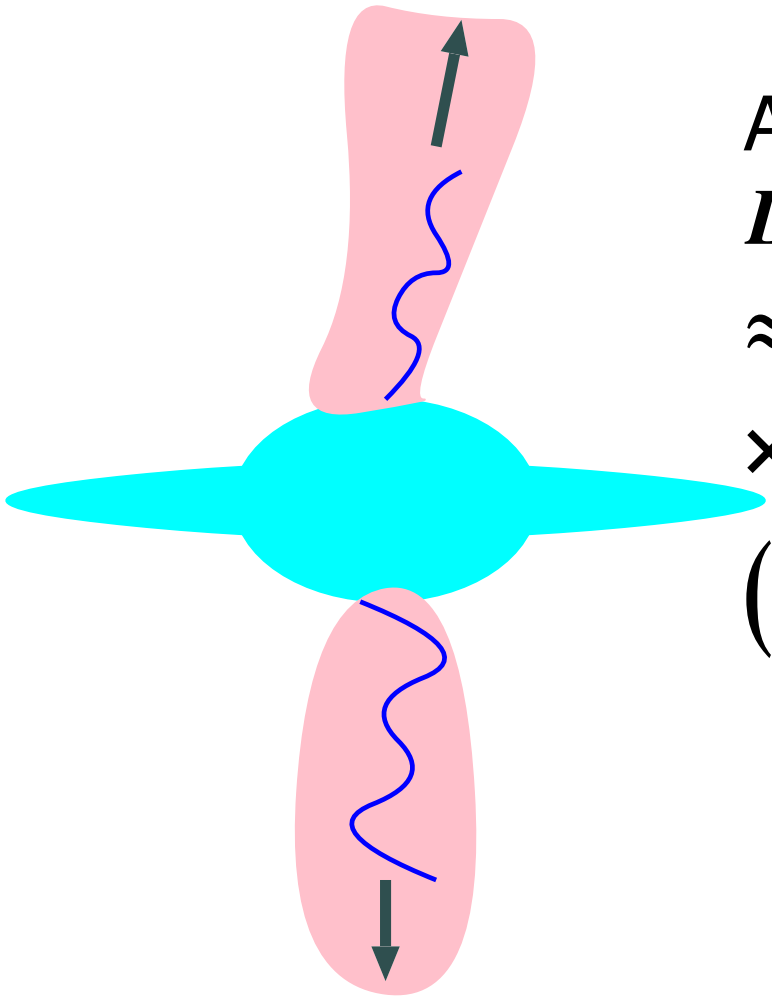

Alfvén wave emission

$$L_{\rm A} \approx 2\pi l^2 \frac{\delta B^2}{8\pi} v_{\rm A}$$

$$\approx 3\times10^{48}\,{\rm erg/yr}$$

$$\times \left(\frac{\delta B}{10\mu{\rm G}}\right)^2 \left(\frac{B}{100\mu{\rm G}}\right) \left(\frac{n}{10^{-2}{\rm cm}^{-3}}\right)^{-1/2}$$

$$\left(\frac{l}{1{\rm kpc}}\right)^2$$

Magnetic Activity – Fermi Bubble ???

- Outflow in Simulation: $\approx 3 \times 10^{48}$erg/yr
- Required Input for Fermi Bubble: $\sim 10^{48}$erg/yr

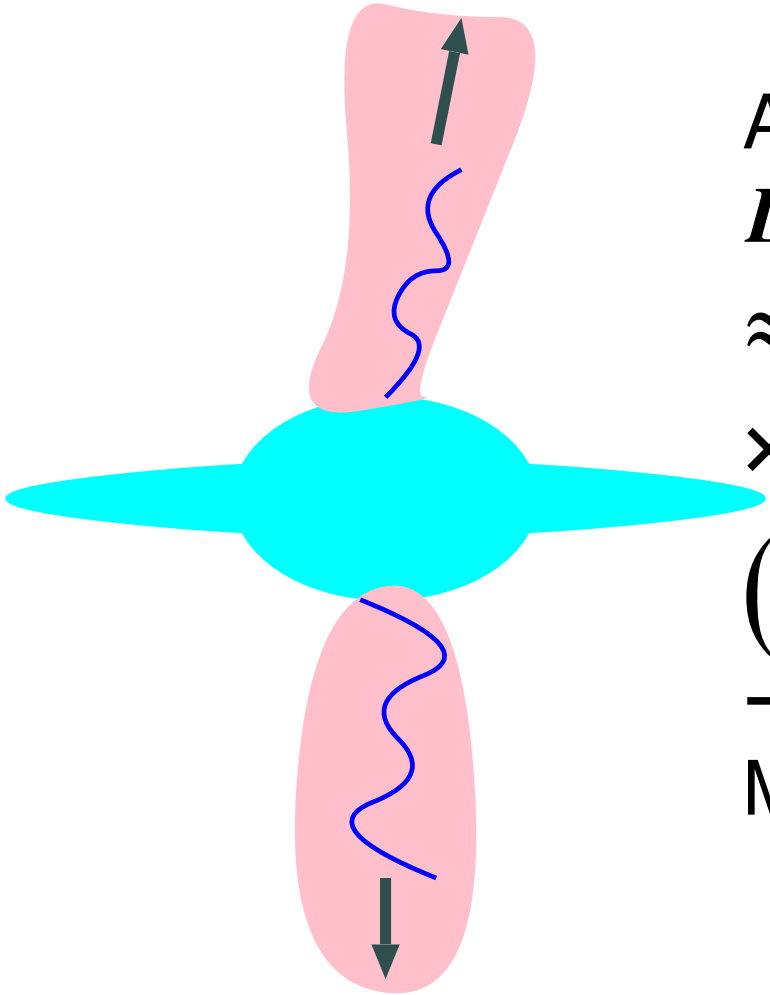

Alfvén wave emission

$$L_A \approx 2\pi l^2 \frac{\delta B^2}{8\pi} v_A$$

$$\approx 3 \times 10^{48} \mathrm{erg/yr}$$

$$\times \left(\frac{\delta B}{10\mu\mathrm{G}}\right)^2 \left(\frac{B}{100\mu\mathrm{G}}\right) \left(\frac{n}{10^{-2}\mathrm{cm}^{-3}}\right)^{-1/2}$$

$$\left(\frac{l}{1\mathrm{kpc}}\right)^2$$

→ dissipation in pre-existing MHD turbulence

Lazarian (2016)

Upward Poynting Flux

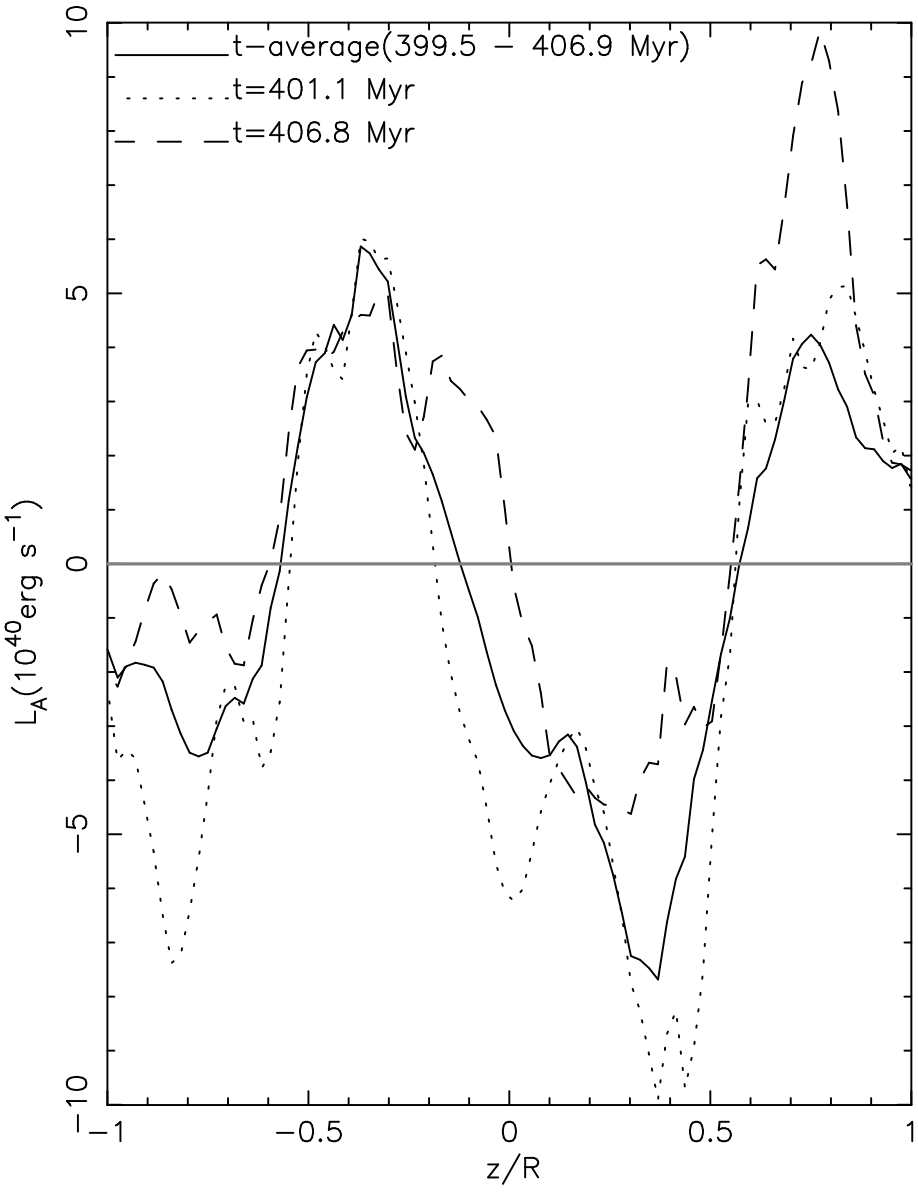

z–L_A (“Alfvénic” Luminosity) inside 1 kpc

$L_A \sim 10^{40} - 10^{41}$erg s^{-1}

$\sim 10^{48}$erg yr^{-1}

Model

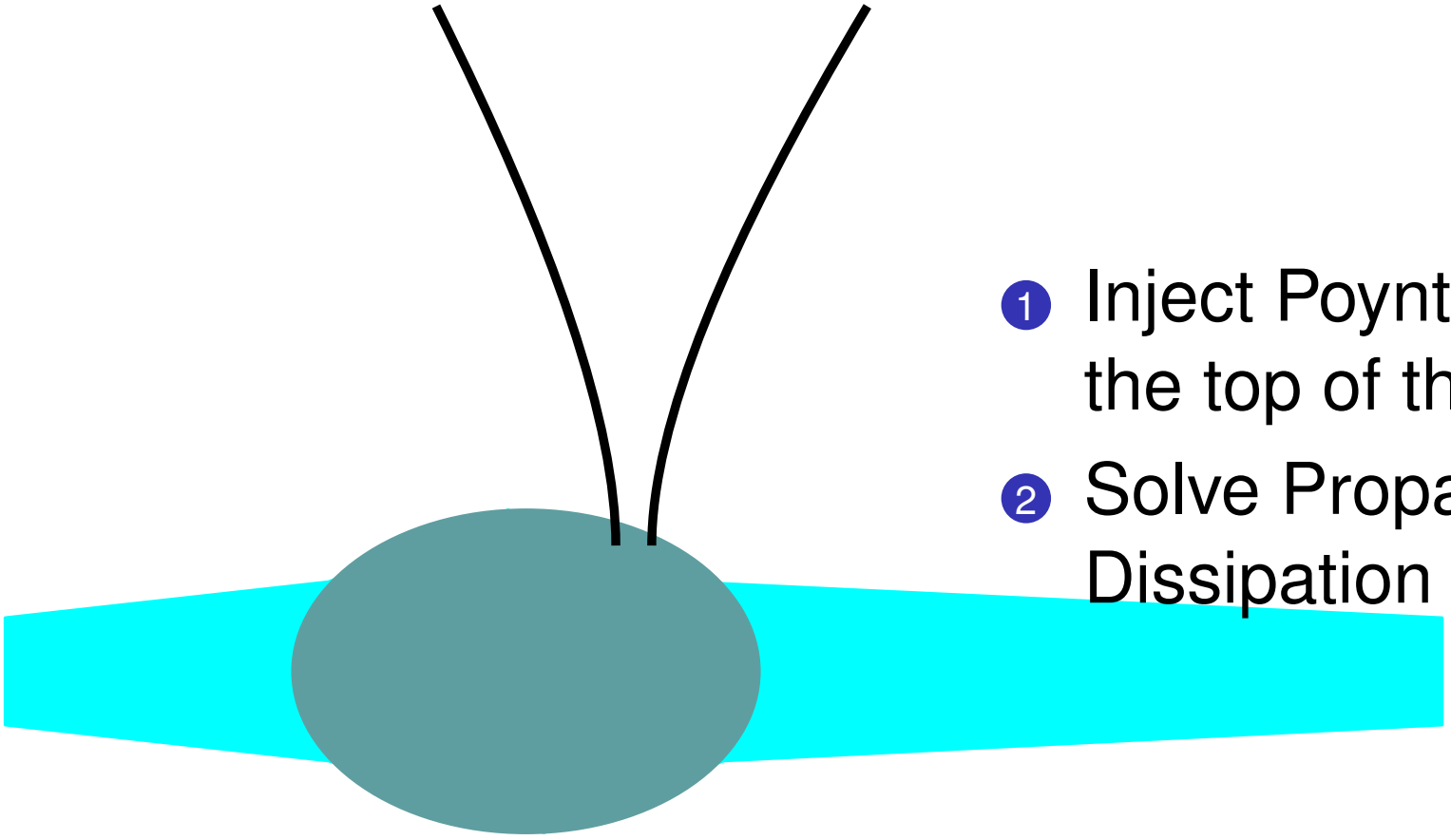

1. Inject Poynting flux from the top of the Bulge.
2. Solve Propagation & Dissipation

Formulation

Hydro + Poynting Flux

$$\frac{d\rho}{dt} + \frac{\rho}{A}\frac{\partial}{\partial z}(Av_z) = 0. \tag{1}$$

$$\rho\frac{dv_z}{dt} = -\frac{\partial}{\partial z}(p_{\rm g} + p_{\rm A}) - \rho\frac{\partial \Phi}{\partial z} = 0, \tag{2}$$

$$\rho\frac{de_{\rm g}}{dt} + \frac{p_{\rm g}}{A}\frac{\partial}{\partial z}(Av_z) = H_{\rm A} \tag{3}$$

$$\rho\frac{d\tilde{e}_{\rm A}}{dt} + \frac{1}{A}\frac{\partial}{\partial z}\left[A\rho\tilde{e}_{\rm A}\left(v_{\rm A} + \frac{1}{2}v_z\right)\right] - \frac{v_z}{2}\frac{\partial}{\partial z}(\rho\tilde{e}_{\rm A}) = -\gamma_{\rm A}\rho\tilde{e}_{\rm A}, \tag{4}$$

where $e_{\rm A} \equiv \frac{1}{2}v_\perp^2 + \frac{B_\perp^2}{8\pi} = v_\perp^2 = \frac{B_\perp^2}{4\pi}$.

Poynting Flux-driven Outflow

Poynting Flux-driven Outflow

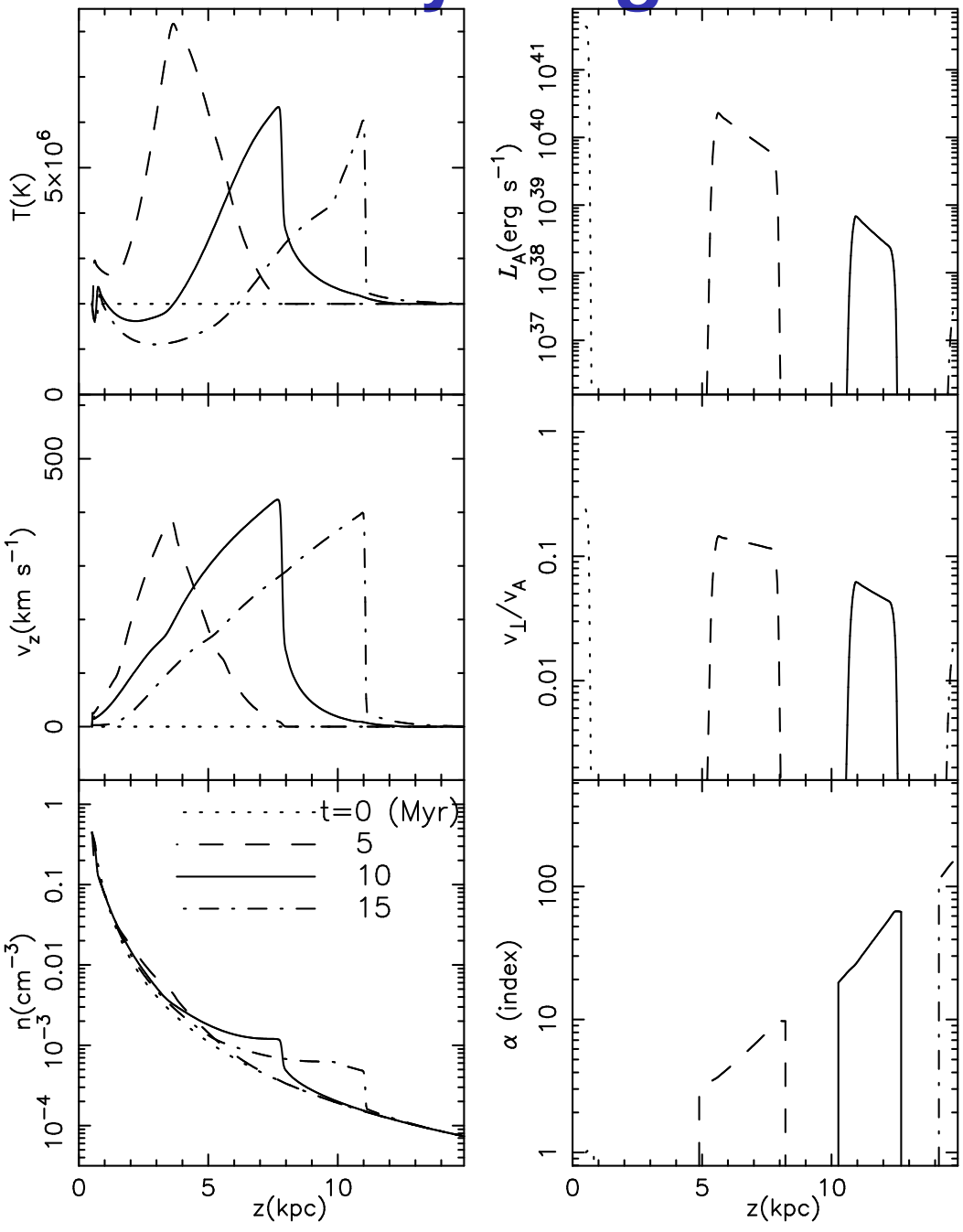

at 10 kpc

- $T \approx 6 \times 10^6$K
- $v \approx 400 - 500$ km s^{-1}
- $n \approx (6-7) \times 10^{-4}$cm^{-3}

$\Leftrightarrow$ Observation

(Miller & Bregman 2016)

Summary

Summary

Global MHD simulation for Bulge + Disk
under Axisymmetric Grav. Pot.

Magnetic Activity ⇒

Summary

Global MHD simulation for Bulge + Disk
under Axisymmetric Grav. Pot.

Magnetic Activity ⇒

- Non-circular Motion

Summary

Global MHD simulation for Bulge + Disk
under Axisymmetric Grav. Pot.

Magnetic Activity ⇒

- Non-circular Motion
- Time-dependent “parallelogram” in l–v diagram by Radial Motion

Summary

Global MHD simulation for Bulge + Disk
under Axisymmetric Grav. Pot.

Magnetic Activity ⇒

- Non-circular Motion
- Time-dependent "parallelogram" in l–v diagram by Radial Motion
- High v feature by Vertical Motion
  ⇐ Magnetic sliding slope via Parker Instability

Summary

Global MHD simulation for Bulge + Disk
under Axisymmetric Grav. Pot.

Magnetic Activity ⇒

- Non-circular Motion
- Time-dependent "parallelogram" in l–v diagram by Radial Motion
- High v feature by Vertical Motion
  ⇐ Magnetic sliding slope via Parker Instability
- Large-scale Outflows

Summary

Global MHD simulation for Bulge + Disk
under Axisymmetric Grav. Pot.

Magnetic Activity ⇒

- Non-circular Motion
- Time-dependent "parallelogram" in l–v diagram by Radial Motion
- High v feature by Vertical Motion
  ⇐ Magnetic sliding slope via Parker Instability
- Large-scale Outflows

Future Extensions

- Realistic Heating/Cooling
- Detailed trajectories of gas clouds

Kruijssen+ 2015; Henshaw+ 2016